Developmental Cell
Article

α-Catenin and IQGAP Regulate Myosin Localization to Control Epithelial Tube Morphogenesis in *Dictyostelium*

Daniel J. Dickinson,[1,6] Douglas N. Robinson,[5] W. James Nelson,[1,2,3,*] and William I. Weis[1,3,4,*]
[1]Program in Cancer Biology
[2]Department of Biology
[3]Department of Molecular and Cellular Physiology
[4]Department of Structural Biology
Stanford University, Stanford, CA 94305, USA
[5]Departments of Cell Biology and Pharmacology and Molecular Sciences, Johns Hopkins University School of Medicine, Baltimore, MD 21205, USA
[6]Present address: Department of Biology, University of North Carolina, Chapel Hill, NC 27599, USA
*Correspondence: wjnelson@stanford.edu (W.J.N.), bill.weis@stanford.edu (W.I.W.)
http://dx.doi.org/10.1016/j.devcel.2012.06.008

SUMMARY

Apical actomyosin activity in animal epithelial cells influences tissue morphology and drives morphogenetic movements during development. The molecular mechanisms leading to myosin II accumulation at the apical membrane and its exclusion from other membranes are poorly understood. We show that in the nonmetazoan *Dictyostelium discoideum*, myosin II localizes apically in tip epithelial cells that surround the stalk, and constriction of this epithelial tube is required for proper morphogenesis. IQGAP1 and its binding partner cortexillin I function downstream of α- and β-catenin to exclude myosin II from the basolateral cortex and promote apical accumulation of myosin II. Deletion of IQGAP1 or cortexillin compromises epithelial morphogenesis without affecting cell polarity. These results reveal that apical localization of myosin II is a conserved morphogenetic mechanism from nonmetazoans to vertebrates and identify a hierarchy of proteins that regulate the polarity and organization of an epithelial tube in a simple model organism.

INTRODUCTION

Morphogenesis is the process that produces functional tissue architectures during development of an organism. Cell migration, shape changes, and differentiation must occur in concert for normal morphogenesis to occur. In animals, morphogenesis often occurs via the reorganization of cells within epithelial sheets (Keller, 2002; Bryant and Mostov, 2008; St Johnston and Sanson, 2011), but it is unclear how individual cell behaviors are coordinated to produce robust tissue shape changes.

Epithelial cells have molecularly distinct apical and basolateral plasma membrane domains and a polarized organization of the cytoskeleton that allow the cells to undergo directional and reproducible morphogenetic movements (Bryant and Mostov, 2008). The adherens junction, containing cadherin transmembrane adhesion molecules and their cytosolic binding partners including α- and β-catenin, is critical for this polarized cell organization and for the structural integrity of the epithelium (Nelson, 2008).

In many animal epithelial tissues, nonmuscle myosin II (hereafter referred to as "myosin") and actin are enriched at the apical membrane where actomyosin contractility generates forces that lead to changes in tissue shape. In planar epithelia, apical actomyosin activity can cause apical constriction, a morphogenetic process in which apical membranes shrink resulting in bending or invagination of the epithelial sheet (Sawyer et al., 2010). Apical constriction occurs during gastrulation in many animal embryos including *Drosophila* (Sweeton et al., 1991), *Caenorhabditis elegans* (Lee and Goldstein, 2003) and sea urchin (Kimberly and Hardin, 1998), and during vertebrate neural tube closure (Baker and Schroeder, 1967). The ability of actomyosin to power apical constriction in planar epithelia has been relatively well described, but the function of actomyosin in tubular epithelia, in which the apical membrane faces the lumen, has been studied less. Epithelial tubes with apical actomyosin are found in the mammalian salivary gland (Masedunskas et al., 2011), pancreas (Bhat and Thorn, 2009), and the developing kidney (Meyer et al., 2004), as well as in the zebrafish neural tube (Gutzman and Sive, 2010). In some cases, apical actomyosin may regulate the size of the lumen by exerting a force that opposes lumen expansion (Gutzman and Sive, 2010; Masedunskas et al., 2011), but it is unclear whether this is a general phenomenon. In addition, how apical actomyosin contributes to the morphogenesis of epithelial tubes is not well understood.

We examined this problem during multicellular development of the social amoeba *Dictyostelium discoideum.* Social amoebae provide insights into the molecular and cellular factors that contributed to the early evolution of animal morphogenesis because of their phylogenetic position as an outgroup to metazoa. *Dictyostelium* amoebae initiate multicellular development

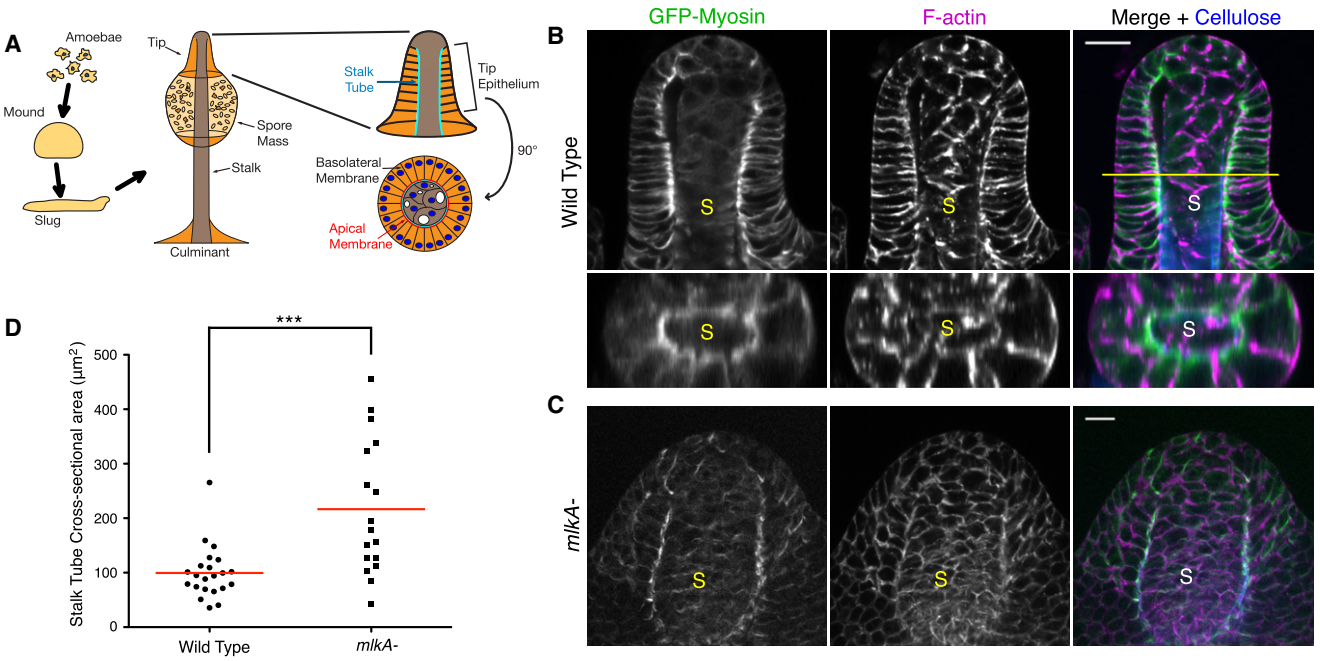

Figure 1. An Apical Actomyosin Ring Constricts the Stalk Tube

(A) Multicellular development and epithelial organization in *D. discoideum*. Upon starvation, cells aggregate to form a mound, which develops into a migrating slug (left). After a period of slug migration, the culminant is formed (center). The tip of the culminant consists of a tubular simple epithelium surrounding the stalk (right). The epithelium and stalk cells are separated by the stalk tube, which is a rigid structure consisting of cellulose and ECM proteins. The apical membrane of the epithelial cells is adjacent to the stalk tube.

(B) Upper panels show a confocal section of the tip of a wild-type culminant expressing GFP-myosin and stained for F-actin and cellulose. Lower panels show a cross-section at the plane indicated by the yellow line in the merged image. S, stalk.

(C) Confocal section of the tip of an *mlkA*− culminant expressing GFP-myosin and stained for F-actin and cellulose.

(D) Quantification of the stalk tube cross-sectional area in wild-type and *mlkA*− culminants. Individual data points are shown, and the line indicates the mean. ***$p < 0.001$ (Mann-Whitney rank sum test).

Scale bars represent 10 μm. See also Figure S1.

by aggregating in response to starvation. In the last stage of development, called culmination, an epithelial tube is formed that surrounds the stalk at the tip of the fruiting body (Figure 1A). Tip epithelial cells have molecularly distinct apical and basolateral plasma membranes, with the apical membrane adjacent to the stalk, and a polarized organization of the plasma membrane, cytoskeleton, and cytoplasmic organelles (Dickinson et al., 2011). The polarity and morphology of the tip epithelium require an α-catenin ortholog and the β-catenin-related protein Aardvark that colocalize to the basolateral plasma membrane, and loss of either of these proteins disrupts epithelial organization and cell polarity.

One important developmental role of the tip epithelium is secretion of cellulose and extracellular matrix (ECM) proteins to form the stalk tube, which is a rigid support that surrounds the stalk cells (Dickinson et al., 2011). The tip epithelium is located close to the substratum at the onset of culmination, but is lifted upward as the stalk forms, depositing cellulose and ECM as it goes (Bonner, 1944; Raper and Fennell, 1952; Bonner et al., 1955). Because of the tubular morphology of the tip epithelium, this secreted material is also organized into a tube. Stalk cells increase in volume approximately 5-fold during culmination, and because these cells are encased in the rigid stalk tube, their expansion is directed upward, which contributes to the lifting force that raises the spore head (Raper and Fennell, 1952). Thus, the patterning of the stalk tube by the tubular tip epithelium is essential for normal culmination in *Dictyostelium* because it allows stalk cell expansion to be converted into a lifting force. Mutations in α-catenin or aardvark (β-catenin) compromise stalk formation by disrupting the organization and polarity of the tip epithelium (Grimson et al., 2000; Coates et al., 2002; Dickinson et al., 2011).

Here, we investigated molecular mechanisms downstream of α-catenin and aardvark (β-catenin) that regulate morphogenesis of the tip epithelial tube. Significantly, as in higher animals, myosin is concentrated at the apical membrane in *Dictyostelium* epithelial cells, where it controls tissue morphology and regulates the size and shape of the lumen (i.e., the stalk). We find that α-catenin regulates the localization of a *Dictyostelium* IQGAP homolog and the actin bundling protein cortexillin, which function together to exclude myosin from the basolateral membrane and promote its accumulation at the apical membrane. Loss of IQGAP1 or cortexillin compromises apical myosin enrichment and disrupts the organization of the epithelial monolayer, but does not affect cell polarity. Our results reveal a hierarchy of actomyosin regulatory proteins that link epithelial cell adhesion, cell polarity and morphogenesis in a simple developmental system.

RESULTS

An Apical Actomyosin Ring Constricts the Stalk in the *Dictyostelium* Tip

To understand the mechanism underlying the organization of tip epithelial cells into a tube during *Dictyostelium* morphogenesis, we began by examining the distribution of myosin in the tip epithelium, because tissue structure is often influenced by myosin activity in metazoans (Kasza and Zallen, 2011). We expressed GFP fused to the N-terminus of myosin heavy chain (Effler et al., 2006). GFP-myosin was expressed at near-endogenous levels, and at comparable levels in all cell lines used in this study (Figure S1 available online). Cortical GFP-myosin was highly enriched at the plasma membrane domain adjacent to the stalk, which corresponds to the apical membrane of the cells, with lesser amounts localized basolaterally (Figure 1B). Myosin colocalized with actin at the apical membrane and formed a continuous ring around the stalk (Figure 1B, lower panels). This structure probably corresponds to the "actin ring" observed in electron micrographs, which consists of bundled actin filaments connected between adjacent cells by electron-dense junctional structures (Grimson et al., 2000; Dickinson et al., 2011). We refer to this structure as the actomyosin ring.

To examine the role of myosin in the organization of the tip epithelium, we interfered with myosin activity. *Dictyostelium* cells that lack myosin heavy chain do not develop past the mound stage (Knecht and Loomis, 1988), precluding an analysis of culmination in these mutants. We therefore sought a milder genetic perturbation that would reduce myosin activity without preventing the cells from reaching culmination. Cells lacking myosin light chain kinase A (*mlkA*-) have reduced myosin activity but are able to complete development (Smith et al., 1996). Culminants of this strain had defects in epithelial organization: the tip epithelium was multilayered, and the cells lacked the elongated, columnar morphology characteristic of wild-type epithelial cells (Figure 1C). Cortical GFP-myosin was still present in these culminants, consistent with the fact that regulatory light chain (RLC) phosphorylation stimulates myosin motor activity but does not affect its actin binding or bipolar thick filament assembly. With the assumption that RLC is the primary substrate of MIkA (Smith et al., 1996), these results indicate that wild-type levels of myosin activity are required for normal organization of the tip epithelium.

The presence of an actomyosin ring surrounding the stalk in the tip epithelium coincides with a previous description of a narrowing of the stalk in this region (Grimson et al., 2000), suggesting that the activity of the apical actomyosin ring in the tip epithelium compresses the stalk. To directly test this hypothesis, we measured the width of the stalk in *mlkA*− culminants. Indeed, loss of *mlkA* caused the stalk to be significantly wider than in wild-type culminants (cross-sectional area mean ± SEM of 220 ± 30 μm^2 for *mlkA*− compared with 100 ± 10 μm^2 for wild-type; Figure 1D). These data strongly suggest that the contractile actomyosin ring in the tip epithelial cells compresses the stalk as it forms, although we cannot formally exclude the possibility that the multilayering of the tip epithelium in *mlkA*− also contributes to stalk expansion. Because tip epithelial cells secrete cellulose and ECM proteins to form a rigid tube that encases the entire stalk (Dickinson et al., 2011), constriction of the stalk in the tip probably restricts the stalk diameter along its entire length, resulting in a long, thin stalk.

β- and α-Catenin Are Required for Apical Myosin Localization and Stalk Constriction

The disruption of epithelial morphology in *mlkA*− culminants is reminiscent of the phenotype observed upon loss of α-catenin or the β-catenin-related protein Aardvark, which are required for epithelial cell polarity in *Dictyostelium* and higher metazoans (Dickinson et al., 2011). We therefore tested whether the catenins regulate myosin localization. We previously characterized two phenotypic classes resulting from α-catenin depletion by RNA interference *ctnnA(RNAi)*: a severe phenotype in culminants lacking detectable α-catenin, in which no trace of epithelial organization is visible; and a milder phenotype resulting from partial α-catenin depletion, in which the epithelial cells are recognizable but epithelial cell polarity and organization are disrupted (Dickinson et al., 2011). We focused on *ctnnA(RNAi)* culminants with the milder phenotype, since these culminants had a recognizable epithelium in which GFP-myosin localization could be analyzed. We also examined mutants lacking aardvark (*aarA*−). In *ctnnA(RNAi)* and *aarA*− culminants, apical localization of GFP-myosin was not uniform and appeared reduced compared to wild-type (Figures 2A and 2B, compare to Figure 1B). We also observed large accumulations of myosin that were not adjacent to the stalk tube (Figures 2A and 2B, arrows). Quantitatively, there was a net redistribution of myosin away from the stalk tube: GFP-myosin levels were reduced apically, but increased along the lateral membrane (Figure 2C; see Figure S2 for an illustration of our measurement procedure). Closer examination revealed that the actomyosin ring was not continuous around the entire stalk (Figures 2A and 2B; arrowheads indicate breaks in the actomyosin ring). Consistent with this disruption of the actomyosin ring, the stalk was significantly wider in *ctnnA(RNAi)* and *aarA*− culminants (cross-sectional area mean ± SEM of 150 ± 17 μm^2 for *ctnnA(RNAi)* and 140 ± 12 μm^2 for *aarA*− compared with 70 ± 10 μm^2 for wild-type; Figure 2D). We conclude that both α-catenin and aardvark are required for the normal distribution of myosin in the tip epithelium and the formation of a functional actomyosin ring that constricts the stalk.

Identification of IQGAP and Cortexillin as α-Catenin-Interacting Proteins

To investigate the molecular mechanism by which the catenins control myosin localization in the tip epithelium, we sought to identify known regulators of myosin activity that interact with α-catenin. We immunoprecipitated α-catenin from fruiting bodies and analyzed the immunoprecipitates by mass spectrometry (Figure 3A; see Experimental Procedures). We chose two isoforms of IQGAP and two isoforms of the actin crosslinker Cortexillin for further study (Figure 3B). IQGAPs form complexes with cortexillins (Faix et al., 2001; Lee et al., 2010), and together these proteins have been implicated in the regulation of myosin distribution in single cells undergoing cytokinesis (Faix et al., 1996, 2001; Adachi et al., 1997; Lee et al., 1997; Weber et al., 1999; Ren et al., 2009; Kee et al., 2012). *D. discoideum* IQGAP proteins contain RasGAP-related domains homologous to those in animal and yeast IQGAPs, but lack the N-terminal actin binding domains and IQ repeats present in metazoan IQGAPs

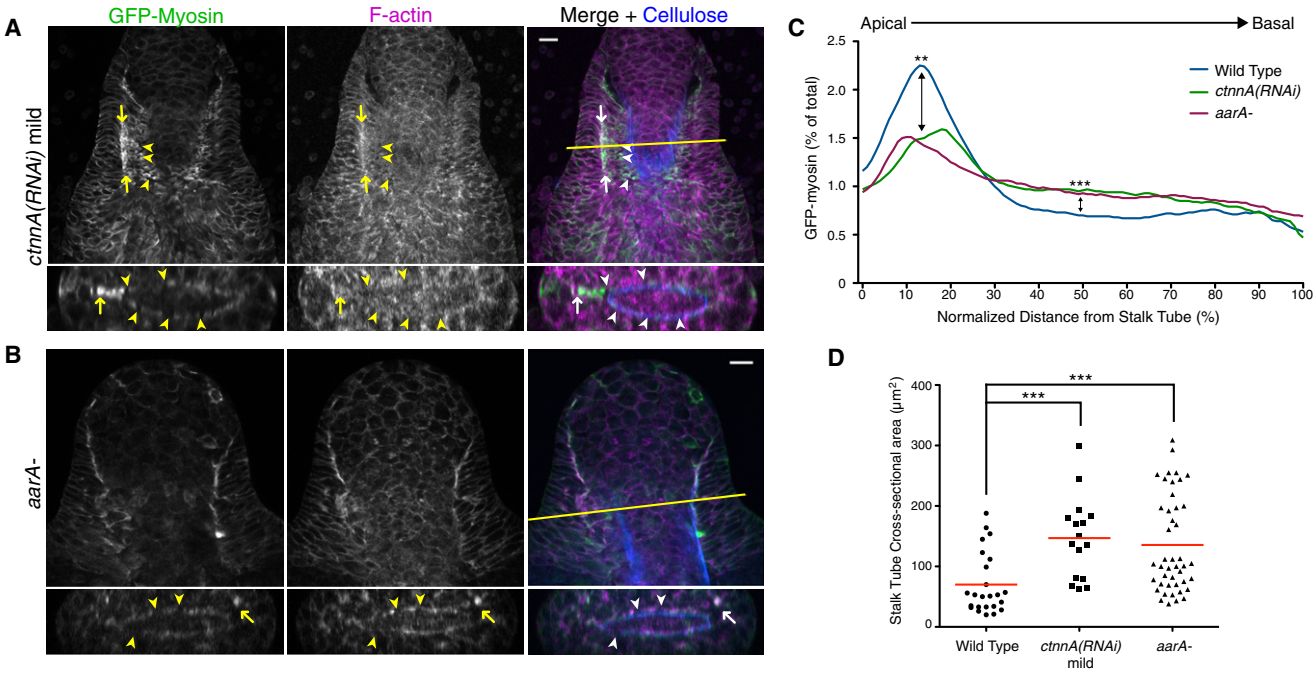

Figure 2. β- and α-Catenin Are Required for Normal Myosin Localization and Stalk Tube Constriction

(A and B) Upper panels show confocal sections of the tips of culminants of the indicated strains expressing GFP-myosin and stained for F-actin and cellulose. Lower panels show cross-sections at the planes indicated by the yellow lines in the merged images. Arrows indicate accumulation of actomyosin distant from the stalk tube. Arrowheads indicate gaps in the actomyosin ring.

(C) Quantification of myosin localization in culminants of the indicated genotypes. GFP-myosin intensity was measured as a function of distance from the stalk tube, and average distributions are shown (n = 27 for wild-type, n = 18 for *ctnnA(RNAi)* and n = 35 for *aarA*−). **p < 0.01 at 15%; ***p < 0.001 at 50% of tip epithelial height (Kruskal-Wallis test with Dunn's posttest). The overall shapes of the distributions are also significantly different (p < 0.001 for both *ctnnA(RNAi)* versus wild-type and *aarA*− versus wild-type; Kolmogorov-Smirnov test).

(D) Quantification of the stalk tube cross-sectional area in the culminants of the indicated genotypes. Individual data points are shown, and the line indicates the mean. ***p < 0.001 (Kruskal-Wallis test with Dunn's posttest).

Scale bars represent 10 μm. See also Figure S2.

(Figure S3). Cortexillins consist of actin binding and coiled-coil domains (Figure S3), and thus likely serve as the actin-binding moiety in the IQGAP-cortexillin complex (see also Figure 5, below).

We examined the localization of IQGAP1 and cortexillins I and II by immunofluorescence. Endogenous IQGAP1 and both cortexillins colocalized with α-catenin at the basolateral cortex of *Dictyostelium* tip epithelial cells (Figures 3C–3E). IQGAP1, cortexillins and α-catenin were notably absent from the apical membrane, where actin and myosin were enriched (Figures 3C–3E, arrowheads; compare to Figure 1B). The colocalization of IQGAP1, cortexillin I, cortexillin II and *Dd*α-catenin at the basolateral membrane is consistent with the possibility that these proteins function together in a complex (Figures 3A and 3B).

IQGAP1 and Cortexillins Control Myosin Localization in the Tip Epithelium

Because IQGAP1 and cortexillins are known to regulate myosin organization in single *Dictyostelium* cells (Ren et al., 2009; Lee et al., 2010), we hypothesized that they regulate myosin in the tip epithelium during culmination. To test this hypothesis, we first examined mutants lacking IQGAP1 (*iqgA*−). In *iqgA*− culminants, tip epithelial organization was severely disrupted (Figure 4A). The epithelium was multilayered and, unlike in wild-type culminants, the epithelial cells were not elongated in the direction perpendicular to the stalk tube. GFP-myosin was not enriched at the plasma membrane adjacent to the stalk tube (Figure 4C), and the actomyosin ring was not visible. As in *ctnnA(RNAi)* and *aarA*− culminants, disruption of the epithelium resulted in a significantly wider stalk tube (160 ± 15 μm^2 for *iqgA*− compared with 81 ±10 μm^2 for wild-type; Figure 4D). A mutant lacking IQGAP2 (*iqgB*−) did not have any developmental phenotype (Adachi et al., 1997), consistent with the very low expression levels of IQGAP2 in culminants (Rot et al., 2009); therefore, IQGAP2 was not examined further.

We next examined culminants lacking cortexillin I (*ctxA*−). *ctxA*− tips appeared disorganized, with gaps in the actomyosin ring and abnormal accumulations of myosin distant from the stalk tube (Figure 4B). Unlike *iqgA*− culminants, most *ctxA*− culminants contained small regions of normally organized epithelium (Figure 4B'), which varied in size (Figure S4). However, GFP-myosin was redistributed basolaterally to a similar extent overall as in *igqA*− culminants (Figure 4C). Moreover, the stalk tube in *ctxA*− mutants was widened to a similar degree as in the *iqgA*− mutants (140 ± 13 μm^2 for *ctxA*− compared with 160 ± 15 μm^2 for *iqgA*− and 81 ± 10 μm^2 for wild-type; Figure 4D), indicating that these small patches of epithelium were not sufficient to constrict the stalk. This result is consistent with our

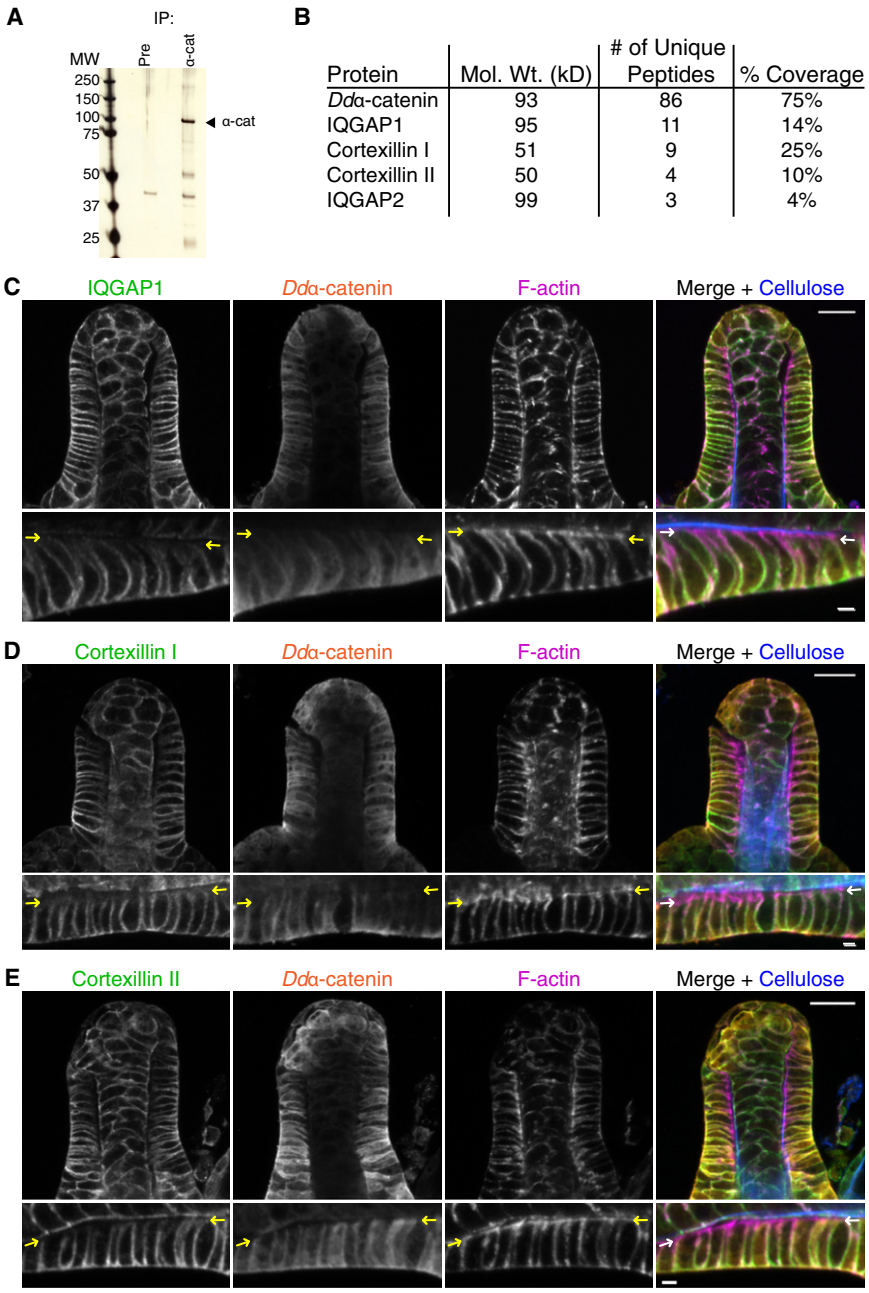

Protein	Mol. Wt. (kD)	# of Unique Peptides	% Coverage
*Dd*α-catenin	93	86	75%
IQGAP1	95	11	14%
Cortexillin I	51	9	25%
Cortexillin II	50	4	10%
IQGAP2	99	3	4%

Figure 3. Identification of IQGAP and Cortexillins as α-Catenin-Interacting Proteins

(A) Whole fruiting body lysates were immunoprecipitated with control or anti-α-catenin antibodies and the resulting samples analyzed by SDS-PAGE and silver staining.

(B) Partial list of proteins identified by LC/MS-MS analysis of an α-catenin immunoprecipitate from whole fruiting bodies.

(C–E) Confocal sections of the entire tip (upper panels) or tip epithelium (lower panels) of wild-type culminants stained as indicated. In the lower panels, the top of the image faces the stalk. Arrows indicate the apical membrane, where actin and myosin are enriched but IQGAP1, cortexillin I and II, and α-catenin are absent. Scale bars represent 10 μm in upper panels and 2 μm in lower panels.

See also Figure S3.

interpretation that a continuous actomyosin ring is essential for the compression of the stalk by the tip epithelial cells. We did not examine culminants lacking cortexillin II (*ctxB*), but importantly, cortexillin II localization was strongly perturbed in *ctxA*− mutants (see below). We therefore interpret the phenotype of *ctxA*− culminants as resulting from a loss of function of both cortexillins.

IQGAP1 and cortexillins colocalized in the tip epithelium (Figure 3), and loss of either IQGAP1 or cortexillin I produced a similar phenotype (Figure 4). This was surprising because *iqgA*− and *ctxA*− have distinct phenotypes in single cells undergoing cytokinesis (Kee et al., 2012). IQGAP1 and cortexillins form a complex in single *D. discoideum* cells (Faix et al., 2001; Lee et al., 2010), and we confirmed that both cortexillins coimmunoprecipitated with GFP-IQGAP1 in wild-type culminants (Figure 5A). To understand why *iqgA*− and *ctxA*− culminants had similar phenotypes, we asked how formation of an IQGAP1/cortexillin complex was related to the function of these proteins. First, we examined cortexillin localization in *iqgA*− culminants. Loss of IQGAP1 strongly reduced the total levels of both cortexillin I and II (Figure 5B), their association with a Triton X-100-insoluble cytoskeletal fraction (Figure 5C), and their cortical localization (Figure 5D). Thus, IQGAP1 is required for normal expression and cortical localization of cortexillins I and II. This is in contrast to single cells in which cortexillin I localizes to the cortex in the absence of IQGAP1 (Faix et al., 2001; Kee et al., 2012) (see Discussion).

Next, we examined IQGAP1 and myosin localization in *ctxA*− culminants. In wild-type cells, IQGAP1 and GFP-myosin had opposite cortical localizations: GFP-myosin was enriched apically (Figure 1B), whereas IQGAP1 localized basolaterally (Figure 3C). Indeed, a pixel-by-pixel analysis demonstrated that the distributions of IQGAP1 and GFP-myosin were anti-correlated in wild-type tip epithelia (Figure 5E). Importantly, this anti-correlation was abolished in *ctxA*− culminants (Figure 5E), and areas of colocalization between IQGAP1 and GFP-myosin were visible in the tip epithelium (Figure 5F). Loss of cortexillin I also reduced the levels of IQGAP1, its recruitment to the cortex and its association with the cytoskeleton (Figures 5B–5D). Two interpretations are consistent with these results. Loss of cortexillin I could cause a redistribution of IQGAP1 from its normal localization opposite of myosin, to lower-affinity cortical sites unrelated to myosin. Alternatively, loss of cortexillin I could reveal a sub-population

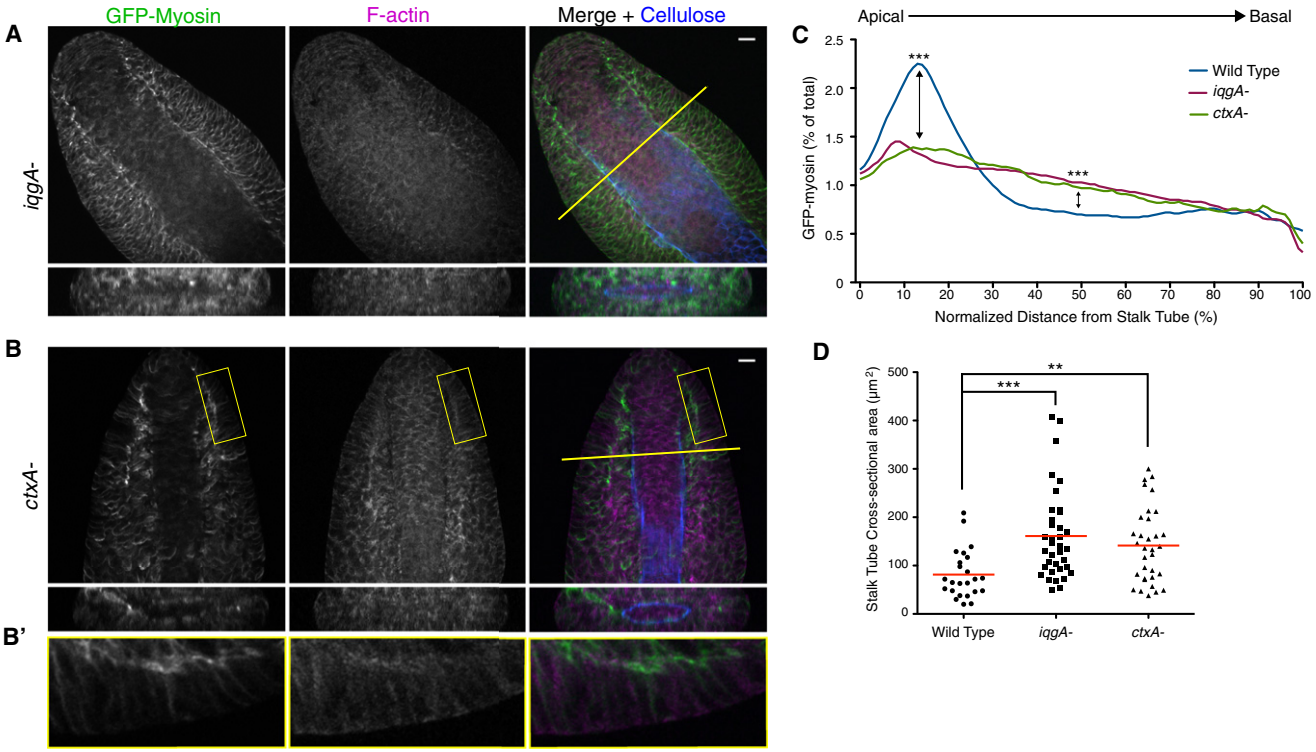

Figure 4. IQGAP1 and Cortexillin I Are Required for Normal Myosin Organization and Tissue Morphology

(A and B) Upper panels show confocal sections of the tips of culminants of the indicated strains, expressing GFP-myosin and stained for F-actin and cellulose. Lower panels show cross-sections at the planes indicated by the yellow lines in the merged images. The image in (B) is representative of the majority of cases; see Figure S4 for the full range of phenotypes observed in this strain.

(B') Enlarged view of the boxed region in (B), showing a small patch of normal epithelium.

(C) Quantification of myosin localization in the indicated strains. GFP-myosin intensity was measured as a function of distance from the stalk tube, and average distributions are shown (n = 27 for wild-type, n = 30 for *iqgA*−, and n = 23 for *ctxA*−). The data from wild-type culminants in Figure 2C are shown again here for comparison. ***p < 0.001 at 15% and 50% of tip epithelial height (Kruskal-Wallis test with Dunn's posttest). The overall shapes of the distributions are also significantly different (p < 0.001 for both *iqgA*− versus wild-type and *ctxA*− versus wild-type; Kolmogorov-Smirnov test).

(D) Quantification of the stalk tube cross-sectional area in the culminants of the indicated genotypes. Individual data points are shown, and the line indicates the mean. **p < 0.01; ***p < 0.001 (Kruskal-Wallis test with Dunn's posttest).

Scale bars represent 10 μm. See also Figure S4.

of IQGAP1 whose localization is unrelated to myosin. In either case, our data strongly suggest that in the tip epithelium, the majority of cortexillin I and a large fraction of IQGAP1 exist in a complex, and that cortical localization of myosin and of the IQGAP1/cortexillin I complex are mutually exclusive.

We also observed that cortical localization of cortexillin II (*ctxB*) was not detectable by immunofluorescence in culminants in which the cortexillin I gene (*ctxA*) was disrupted (Figure 5D). Cortexillin II was expressed at normal levels in *ctxA*− culminants (Figure 5B) but was not associated with the cytoskeleton (Figure 5C). In previous studies, cortexillin II coimmunoprecipitated with IQGAP1 in wild-type cells (Lee et al., 2010; see also Figure 5A) but not in cells lacking cortexillin I (Faix et al., 2001), indicating that cortexillin I is required to recruit cortexillin II into a complex containing IQGAP1. These results are consistent with our finding that IQGAP1 is necessary for recruitment of both cortexillins to the basolateral cortex of tip epithelial cells. In summary, our results support the existence of a protein complex containing IQGAP1, cortexillin I, and cortexillin II in tip epithelial cells; for simplicity, we refer to this complex as IQGAP1/cortexillin. The redistribution of GFP-myosin to the basolateral cortex in *iqgA*− and *ctxA*− culminants (Figure 4C) indicates that the mutually exclusive cortical localizations of GFP-myosin and IQGAP1/cortexillin in wild-type culminants is at least partially due to inhibition of myosin cortical localization by IQGAP1/cortexillin, although we do not exclude the possibility that myosin may also influence IQGAP1/cortexillin localization by a feedback mechanism.

Aardvark and α-Catenin Control the Localization of IQGAP1/Cortexillin

Since we found that IQGAP1 and cortexillins interact with α-catenin (Figure 3) and produce similar epithelial organization defects, we examined the functional relationship between IQGAP1/cortexillin and the catenins. In *ctnnA(RNAi)* and *aarA*− culminants, IQGAP1 and cortexillin I were localized to the apical membrane adjacent to the stalk tube in some cells (Figures 6A, 6B, 6D, and 6E, arrows), a localization that was not observed in wild-type epithelial cells (Figures 3C–3E). The ratio of apical to basal intensity of both IQGAP1 and cortexillin I was increased

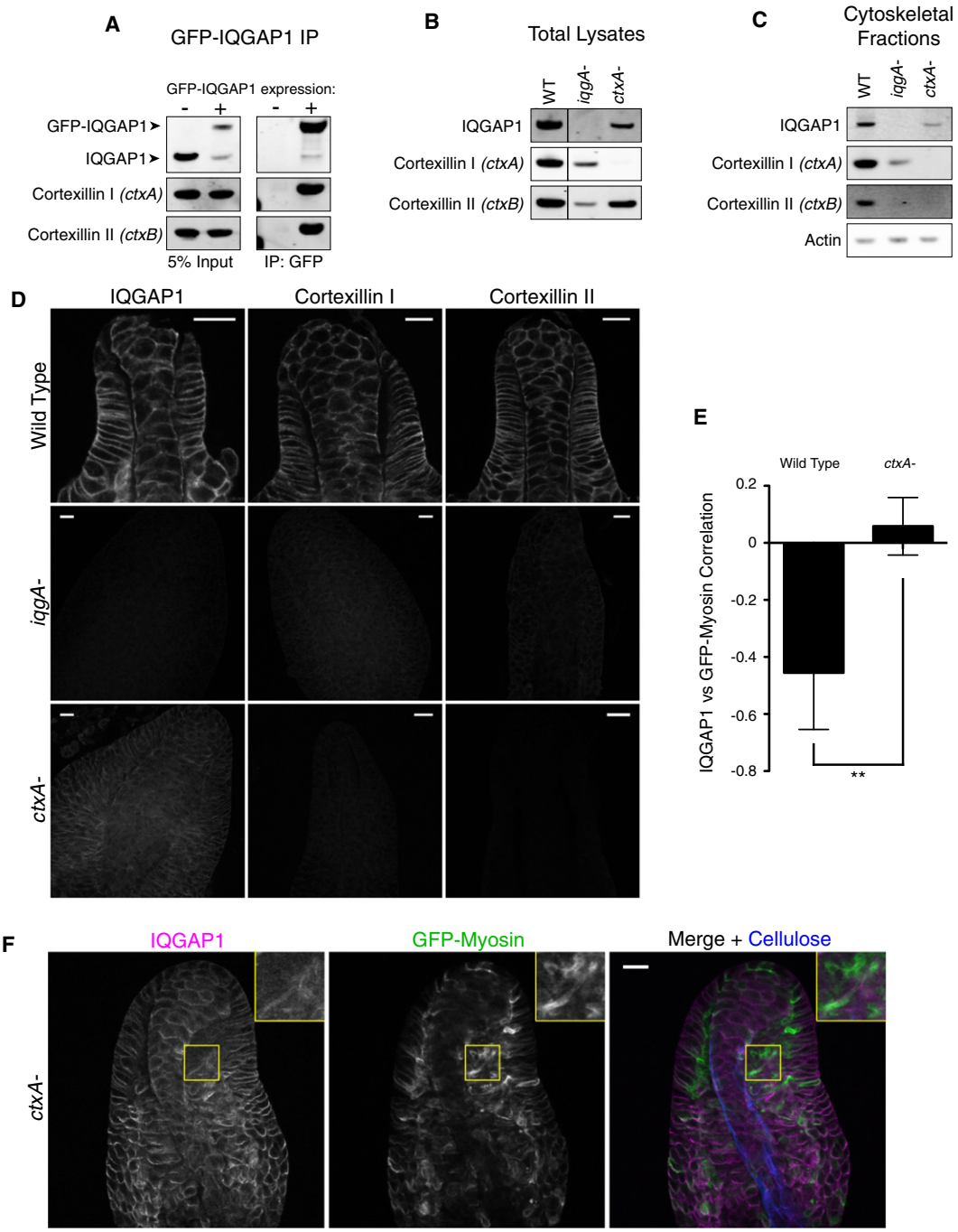

Figure 5. IQGAP1 and Cortexillins Function in a Complex

(A) Coimmunoprecipitation experiment demonstrating interaction of cortexillins I and II with GFP-IQGAP1 in culminants.

(B) Lysates from culminants of the indicated strains were separated by SDS-PAGE and analyzed by western blotting with the indicated antibodies. Equal numbers of cells were loaded in each lane. The vertical line shows where the blots were cropped to remove an irrelevant lane.

(C) Triton-insoluble cytoskeletons were isolated from culminants of the indicated strains and analyzed by western blotting with the indicated antibodies.

(D) Confocal sections of the tips of culminants of the indicated genotypes, stained as indicated. The three samples shown in each column were stained in parallel, and the images were collected and processed using identical settings, allowing intensities to be directly compared.

(E) Correlation of GFP-myosin and IQGAP1 localization in epithelia of the indicated genotypes. Negative values of the correlation coefficient indicate that localization of the two proteins is mutually exclusive. Error bars indicate 95% confidence intervals. **$p < 0.001$ (Kruksal-Wallis test with Dunn's posttest). $n = 6$ for wild-type and $n = 16$ for *ctxA*−.

(F) Confocal section of the tip of a *ctxA*− culminant expressing GFP-myosin and stained for IQGAP1 and cellulose. The IQGAP1 image was adjusted for easy visibility, and thus appears brighter than the comparable image in (D). Insets show enlarged views of the boxed regions.

Scale bars represent 10 μm.

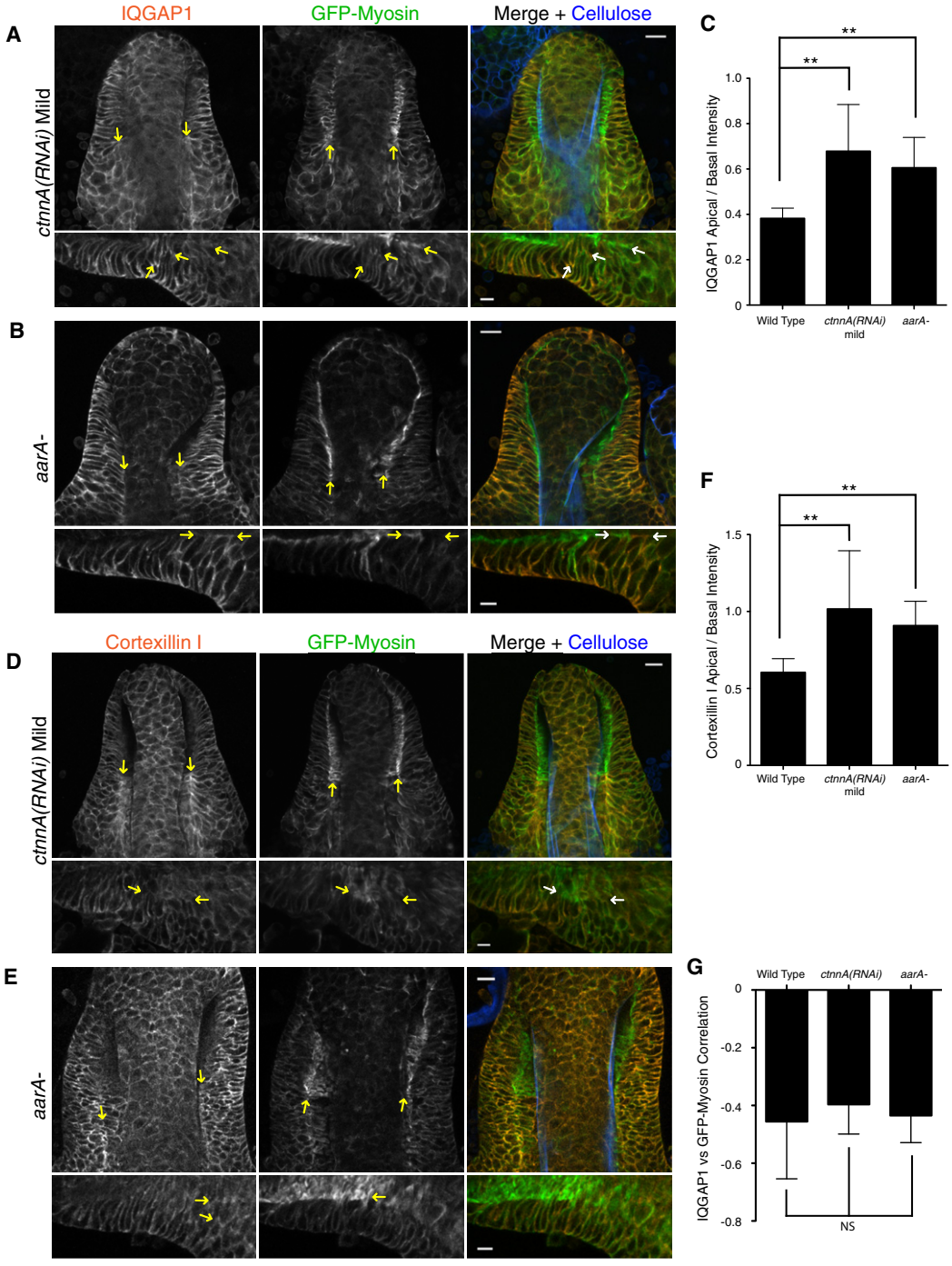

Figure 6. IQGAP1/Cortexillin Localization Is Opposite Myosin and Is Controlled by β- and α-Catenin

(A, B, D, and E) Confocal sections of the tip (upper panels) or tip epithelium (lower panels) of culminants of the indicated genotypes, expressing GFP-myosin and stained as indicated. Arrows indicate reciprocal localization of GFP-myosin and IQGAP1 or cortexillin I. Scale bars represent 10 μm in images of the entire tip and 5 μm in images of the tip epithelium.

(C) Quantification of IQGAP1 localization in epithelia of the indicated genotypes. The ratio of apical:basal staining intensity is shown. **$p < 0.01$ (Kruskal-Wallis test with Dunn's posttest). n = 19 for wild-type, n = 8 for *ctnnA(RNAi)*, and n = 17 for *aarA*−.

(F) Quantification of cortexillin I localization in epithelia of the indicated genotypes. The ratio of apical:basal staining intensity is shown. **$p < 0.01$ (Kruskal-Wallis test with Dunn's posttest). n = 23 for wild-type, n = 6 for *ctnnA(RNAi)*, and n = 20 for *aarA*−.

(G) Correlation of GFP-myosin and IQGAP1 localization in epithelia of the indicated genotypes. Negative values of the correlation coefficient indicate that localization of the two proteins is mutually exclusive. NS, not significant (Kruskal-Wallis test with Dunn's posttest). n = 6 for wild-type, n = 13 for *ctnnA(RNAi)*, and n = 15 for *aarA*−. The data from wild-type in Figure 5E are shown again here for comparison.

Error bars indicate 95% confidence intervals. See also Figure S5.

about two-fold in catenin mutants (Figures 6C and 6F). Importantly, however, the anticorrelation between IQGAP1 and GFP-myosin localization was maintained: apical membranes containing IQGAP1 and cortexillin I lacked bright GFP-myosin fluorescence (Figures 6A, 6B, 6D, and 6E, arrows; quantified in Figure 6G). We conclude that the catenins are required for normal localization of IQGAP1/cortexillin to the basolateral membrane but not for its antagonistic relationship with myosin.

Until now, we have considered only the milder phenotypic class resulting from partial α-catenin depletion by RNAi. We also examined severe *ctnnA(RNAi)* culminants that do not form a recognizable tip epithelium and in which α-catenin is not detectable by immunofluorescence. In the tips of these culminants, IQGAP1 and cortexillin I were cortically localized with a distribution that appeared uniform (Figures S5A and S5B). GFP-myosin again was not colocalized with IQGAP1/cortexillin or, surprisingly, with cortical F-actin; instead, it was concentrated in unusual arc-shaped structures located in the cytoplasm (Figures S5A–S5C). These data support our conclusion that IQGAP1/cortexillin antagonizes the cortical localization of myosin and confirm that α-catenin is not required for this function.

IQGAP1 and Cortexillin Are Not Required for All Aspects of Catenin Function

To further define the relationship between IQGAP1/cortexillin and the catenins, we tested whether loss of IQGAP1 or cortexillin I affected α-catenin localization. Loss of aardvark (β-catenin) strongly reduced α-catenin localization to lateral cell-cell contacts (Figures 7A and 7B), as previously reported (Dickinson et al., 2011). In contrast, lateral membrane localization of α-catenin was clearly visible in *iqgA*− and *ctxA*− epithelial cells, despite the disruption in epithelial morphology (Figure 7A). Quantitatively, the lateral cortical localization of α-catenin appeared slightly reduced in *iqgA*− and *ctxA*− culminants, but this reduction was much less than that in *aarA*- mutants and was not statistically significant (Figure 7B). Total levels of α-catenin were similar in all four of these strains (Figure 7C). We conclude that IQGAP1 and cortexillin I are not essential for normal localization of α-catenin to lateral cell-cell contacts in the tip epithelium.

In addition to effects on tissue organization and myosin distribution, loss of α-catenin or aardvark disrupts epithelial cell polarity and compromises the ability of cells to secrete cellulose and ECM proteins into the stalk tube (Dickinson et al., 2011). We asked whether loss of IQGAP1 or cortexillin I caused a similar loss of cell polarity. Surprisingly, centrosomes were normally localized apically to the nuclei in *iqgA*− and *ctxA*− culminants, even in regions of the epithelium that were multilayered (Figure 7D). Significantly, cellulose synthase (mRFP-DcsA, a marker of the apical plasma membrane; Dickinson et al., 2011) was correctly localized on the plasma membrane closest to the stalk, even in cells that did not contact the stalk tube (Figure 7E). This apical localization of cellulose synthase was associated with adjacent extracellular deposition of cellulose within the epithelium, indicating that cells throughout the multilayered epithelium in *iqgA*− and *ctxA*− culminants were able to secrete stalk tube components apically. Since α-catenin and aardvark are required for the polarized distribution of centrosomes and cellulose synthase in the tip epithelium (Dickinson et al., 2011), these data indicate that the catenins remain functional in *iqgA*− and *ctxA*− mutants, consistent with the normal localization of α-catenin described above. We conclude that although IQGAP1 and cortexillin I are required for normal apical enrichment of myosin in the tip epithelium, these proteins are not required for other aspects of epithelial cell polarity mediated by the catenins.

DISCUSSION

In this study, we showed that myosin is enriched at the apical plasma membrane adjacent to the stalk tube in *Dictyostelium* tip epithelial cells, where it forms a contractile actomyosin ring that constricts the stalk tube. α-Catenin and the β-catenin-related protein aardvark are essential for proper localization of myosin, and we defined a pathway downstream of the catenins that specifies the apical localization of myosin by regulating the distribution of an antagonistic IQGAP1/cortexillin complex. The localization of myosin in the tip epithelial cells is strikingly similar to the apical enrichment of myosin that often occurs during epithelial morphogenesis in higher animals. Topologically, the stalk is equivalent to the lumen of tubular epithelia in animals, so compression of the stalk by the tip epithelium may be analogous to the regulation of luminal volume by apical contractility in epithelia of animals (Gutzman and Sive, 2010; Masedunskas et al., 2011). Thus, our results indicate that apical enrichment of myosin may be a conserved morphogenetic mechanism from social amoebae to animals.

In order to exert a force that can compress the stalk, actomyosin bundles must be interconnected between cells in the epithelial sheet to form a continuous ring. This connection is most likely provided by actin-associated cell-cell junctions that have been observed in electron micrographs of the apical region of the tip epithelium (Grimson et al., 2000; Dickinson et al., 2011). By integrating cytoskeletal force-producing elements across cells in the epithelial sheet, *Dictyostelium* cell-cell junctions may fulfill a function similar to the adherens junction in *Drosophila* (Dawes-Hoang et al., 2005; Martin et al., 2010) and other metazoa. However, it is noteworthy that these *Dictyostelium* cell-cell junctional structures require neither α-catenin nor aardvark, and are unlikely to be molecularly homologous to the adherens junction (Dickinson et al., 2011). It will be important in the future to determine the molecular composition of *Dictyostelium* cell-cell junctions in order to clarify the evolutionary relationship between apical actomyosin contractility in *Dictyostelium* and in metazoans.

In all of the mutants we studied, disruption of the apical actomyosin ring was associated with loss of the monolayer organization of the tip epithelium, raising the question of how apical actomyosin contractility is related to the formation of an epithelial monolayer. One important consideration is cell shape: wild-type epithelial cells are wedge-shaped (narrower at the apical than at the basal surface; Figure 1B, bottom panels) as a necessary consequence of the packing of a monolayer of cells into the cylindrical geometry of the tube. This shape could be the result of apical actomyosin contractility that narrows the apical membrane, analogous to apical constriction in animal epithelial cells. Apical myosin may also help to offset the mechanical stress that results from the local higher curvature along the apical surface relative to the basolateral surface (Borghi and Nelson,

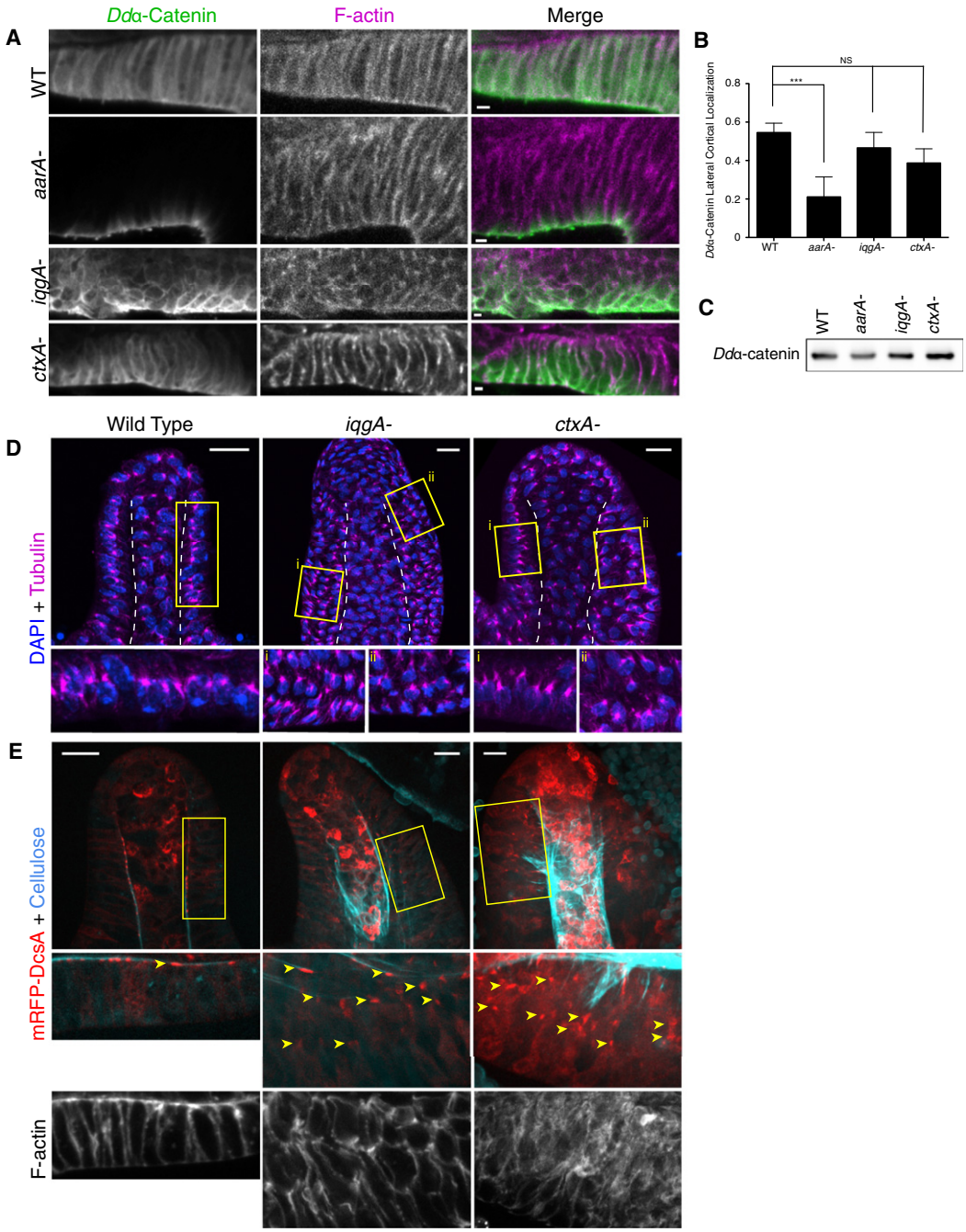

Figure 7. Loss of IQGAP1 or Cortexillin I Does Not Compromise All Aspects of α-Catenin Function

(A) Confocal sections of the tip epithelium in culminants of the indicated genotypes, stained for α-catenin and F-actin. The images shown were derived from samples stained in parallel, and the α-catenin channel was imaged and displayed with identical settings to allow intensities to be directly compared.

(B) Quantification of the cortical localization of α-catenin at the lateral membrane in tip epithelia of the indicated genotypes (see Experimental Procedures). ***$p < 0.001$; NS, not significant (Kruskal-Wallis test with Dunn's posttest). n = 16 for wild-type and *aarA*−, n = 18 for *iqgA*−, and n = 20 for *ctxA*−. Error bars indicate 95% confidence intervals.

(C) Lysates from culminants of the indicated strains were separated by SDS-PAGE and analyzed by western blotting with anti-*Dd*α-catenin. Equal numbers of cells were loaded in each lane.

(D) Maximum intensity projections through the tips of culminants of the indicated genotypes. The samples were stained with DAPI to visualize nuclei and anti-α-tubulin to visualize centrosomes. Lower panels show enlarged versions of the boxed regions, with the top of the images facing the stalk.

(E) Upper panels show maximum intensity projections through the tips of culminants of the indicated genotypes, expressing mRFP-cellulose synthase (DcsA) and stained for cellulose. Middle panels show enlarged versions of the boxed regions, with the top of the images facing the stalk. Lower panels show F-actin staining in single confocal sections of the corresponding regions. Arrowheads indicate apical localization of mRFP-DcsA in cells distant from the stalk.

Scale bars represent 2 μm in (A) and 10 μm in (C–E).

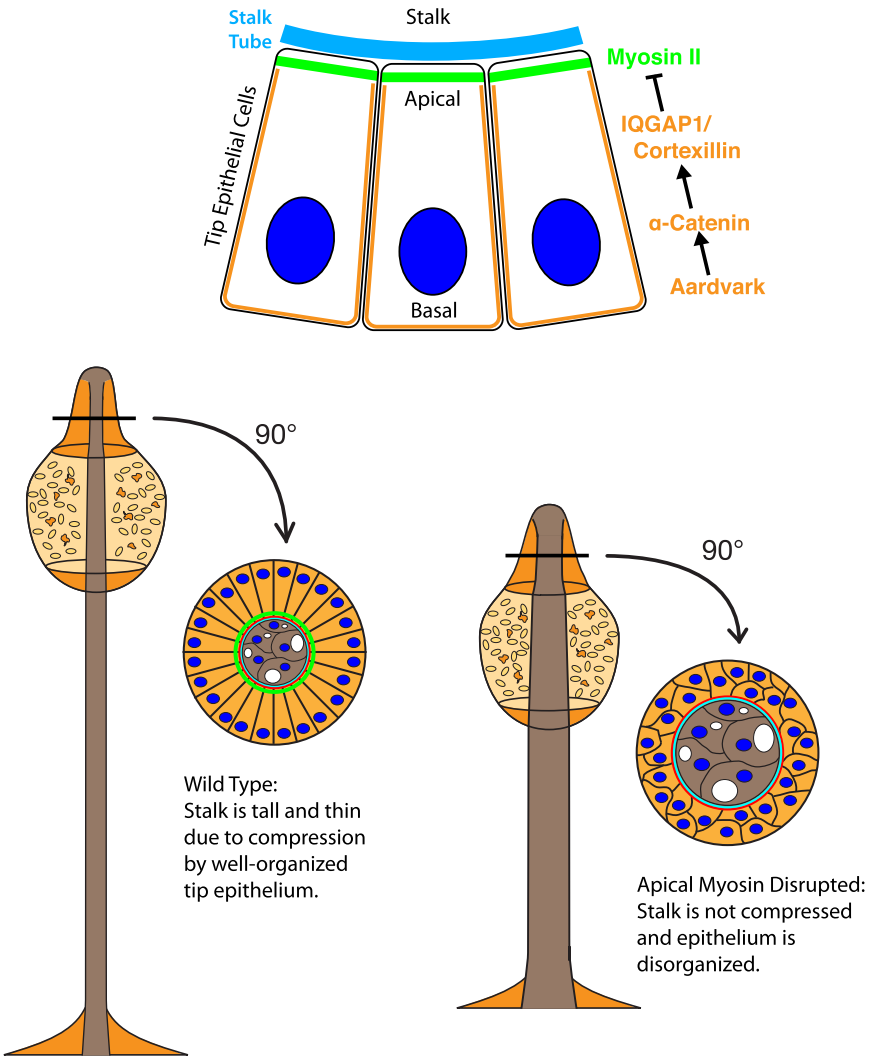

Figure 8. Model of Myosin Regulation during *Dictyostelium* Culmination

In tip epithelial cells, apical myosin localization is enforced by IQGAP1 and cortexillins, which together inhibit the association of myosin with the basolateral cortex. α-Catenin and aardvark control the asymmetric distribution of IQGAP1 and cortexillins, which antagonize cortical myosin recruitment. Apical myosin enrichment is necessary to constrict the stalk and for the normal monolayer organization of the tip epithelium.

2009). The mechanical stress itself might drive myosin to the apical cortex due to the propensity of myosin to accumulate in a mechanosensitive manner (Ren et al., 2009; Luo et al., 2012). At the basolateral surface, IQGAP1/cortexillin and the catenins might rigidify the cortex to help maintain shape. Because myosin, cortexillin I and IQGAP1 contribute to several aspects of cortical mechanics (measured in single cells; Surcel et al., 2010; Kee et al., 2012), it is perhaps not surprising that these proteins have significant impact on epithelial cell and tissue morphology.

A model for the regulation of myosin activity by the catenins and IQGAP1/cortexillin is presented in Figure 8. In the tip epithelium, the IQGAP1/cortexillin complex antagonizes myosin at the basolateral cortex, thereby restricting myosin accumulation to the apical plasma membrane where IQGAP1/cortexillin is absent. The catenins restrict the spatial distribution of IQGAP1/cortexillin to the basolateral plasma membrane, allowing enrichment of myosin apically. In the absence of α-catenin, IQGAP1 and cortexillin occupy the entire cortex, and myosin appears to be excluded from the cortex (Figure S5). This result indicates that α-catenin is not required simply to recruit IQGAP1 and cortexillins to the plasma membrane. Instead, we propose that α-catenin increases the affinity of IQGAP1/cortexillin for the basolateral cortex, perhaps by altering the organization or structure of actin filaments. Alternatively, by influencing membrane trafficking events (Dickinson et al., 2011), α-catenin may cause the asymmetric localization of another factor that affects IQGAP1/cortexillin localization. The small GTPases Rac1 and RacE, which bind IQGAP1 (Faix et al., 1998), are candidates for such a factor.

Our model is based in part on the epithelial phenotypes of *ctnnA(RNAi), aarA−*, *iqgA−*, *ctxA−*, and *mlkA−* culminants, so we considered whether defects occurring at earlier stages of development could contribute to these phenotypes. Several observations argue against this possibility. First, no gross defects in slug formation (the stage immediately preceding culmination) were seen in any of the mutants that we studied (D.J.D., unpublished data). Second, culmination can occur normally under environmental conditions that eliminate the slug stage entirely (Newell et al., 1969), indicating that culmination is not critically dependent on events that occur during the slug stage. Third, *Dictyostelium* development prior to culmination is driven mainly by chemotactic cell migration (Weijer, 2004), and *iqgA−* and *ctxA−* single mutants do not have strong cell migration defects (Lee et al., 2010). Together, these observations support our interpretation of phenotypes observed in epithelial cells as arising during culmination.

Our description of cortexillin I as part of a myosin-antagonizing complex in the tip epithelium might appear to contrast with its role in cytokinesis, where its actin cross-linking activity is essential for a mechanical feedback loop that enhances myosin recruitment both to the cleavage furrow and to sites of ectopic cortical deformation (Ren et al., 2009; Surcel et al., 2010). However, the cortexillin I-binding protein IQGAP1 has been described as an inhibitor of cortical myosin recruitment in both systems (Kee et al., 2012; this work). The apparent difference in cortexillin I function in the tip epithelium compared to single cells likely reflects differential protein abundance: our data

suggest that nearly all of the cortical cortexillin I in tip epithelial cells is bound to IQGAP1 (Figures 5C and 5D), whereas an IQGAP1-free pool of cortexillin I is present in single cells (Faix et al., 2001; Kee et al., 2012) and cooperates with myosin during cytokinesis. Another possible modulator of cortexillin I function is IQGAP2, which is essential for cytokinesis but not for culmination (Adachi et al., 1997) and is expressed at low levels in culminants (Rot et al., 2009). IQGAP2 antagonizes IQGAP1 and promotes cortexillin I-mediated mechanosensing and myosin accumulation at the cleavage furrow (Kee et al., 2012). Therefore, the low abundance of IQGAP2 during culmination might explain why most cortexillin I was found in a myosin-antagonizing complex with IQGAP1. These possibilities are not mutually exclusive, and future studies will seek to define the physical and functional interactions between α-catenin, myosin and IQGAP/cortexillin complexes.

The disruption of apical myosin localization upon loss of α-catenin or aardvark is perhaps not surprising, since the catenins are essential for epithelial polarity in *Dictyostelium* (Dickinson et al., 2011). A more interesting finding is that loss of IQGAP1 or cortexillin I disrupts apical myosin localization without globally affecting cell polarity. This result implicates IQGAP1/cortexillin as a signal transducer that translates cellular polarity into an asymmetric organization of the actomyosin machinery. Disruption of this complex decouples cytoskeletal organization from cell polarity, resulting in a loss of tissue organization. To our knowledge, a similar role for IQGAP in coupling cell polarity to actomyosin organization has not been reported in other systems. However, such a role is plausible, as IQGAP localizes to cell-cell contacts and regulates cell-cell adhesion in both mammalian tissue culture cells (Kuroda et al., 1998; Li et al., 1999) and *Xenopus* embryos (Yamashiro et al., 2007). Determining whether IQGAP controls myosin localization or activity in animal epithelia may reveal mechanisms of tissue organization that have been conserved since the last common ancestor of *Dictyostelium* and metazoans.

EXPERIMENTAL PROCEDURES

Detailed descriptions of strains, plasmids, antibodies, cell culture techniques and quantitative image analysis methods may be found in the Supplemental Experimental Procedures.

Cell Culture, Transformation, and Development

Dictyostelium discoideum cells were cultured in HL5 medium using standard cell culture technique (Fey et al., 2007) and were transformed as described (Gaudet et al., 2007) (see Supplemental Experimental Procedures for details). For development, cells were washed three times in ice-cold development buffer (DB; 5 mM Na_2HPO_4, 5 mM KH_2PO_4, 2 mM $CaCl_2$, 2 mM $MgCl_2$), counted and resuspended in DB. The cells were deposited on 25 mm Whatman Nuclepore filters (0.45 μm pore size) resting on Whatman No. 3 filters soaked with DB. The cell density was 5×10^6 cells per filter. The plates were sealed and development was monitored using a dissecting microscope.

Fluorescence Microscopy

Fluorescence imaging was performed as described (Dickinson et al., 2011). Briefly, cells were developed until culmination and fixed in ethanol containing 4% formalin for 1 hr at 4°C. The specimens were rehydrated in PBS, permeabilized with 1% saponin, and stained sequentially with primary and secondary antibodies. To visualize F-actin, fluorescent phalloidin was added to the secondary antibody solutions. To visualize cellulose, calcofluor (fluorescence brightener 28, MPI Biomedicals) was added to the mounting medium at a final concentration of 200 μg/ml. Specimens were examined with a Zeiss LSM510 confocal microscope equipped with a 63X, 1.4 NA objective. Confocal stacks were assembled and processed using custom-written scripts in ImageJ. When preparing figures for publication, some images were processed with a 3 × 3 median filter to reduce noise, and brightness and contrast were adjusted for easy visibility where appropriate. No other image manipulations were performed.

Image Data Analysis and Statistics

All image measurements were made using ImageJ (see below and Supplemental Experimental Procedures for details). Data analysis, graphing, and statistical tests were performed using Prism (GraphPad Software) and OpenOffice.org Calc (Apache Software Foundation). p values were generated using statistical tests as stated in the figure legends. All error bars indicate 95% confidence intervals unless otherwise specified.

Stalk cross-sectional area was measured from the cellulose channel of an XZ image reconstructed from a 3D confocal series of the tip. The measurement was made at the center (in the vertical direction) of the tip. GFP-myosin distribution was quantified using a procedure equivalent to an average of line scans perpendicular to the stalk tube, as illustrated in Figure S2 and described in Supplemental Experimental Procedures. IQGAP1 and cortexillin I intensities were measured using line scans and are reported as a ratio of apical:basal intensity. To compare IQGAP1 and GFP-myosin distributions, individual pixel intensities were measured and Spearmann's rank correlation coefficient was calculated. To quantify α-catenin cortical localization, colocalization with F-actin (a marker of the cortex) was measured using correlation analysis. The detailed procedures for each of the above measurements are described in the Supplemental Experimental Procedures.

Immunoprecipitation and Mass Spectrometry

To prepare samples for mass spectrometry, cells were developed until culmination was complete, and whole fruiting bodies were dissolved in lysis buffer (25 mM HEPES pH 7.4, 150 mM NaCl, 3 mM EDTA, 1 mM EGTA, 1% Triton X-100) containing the following protease inhibitors: 1 mM AEBSF, 0.5 μg/ml Antipain, 0.5 μg/ml Aprotinin, 0.5 μg/ml BAEE, 1 mM Benzamidine, 5 μg/ml Chymostatin, 10 μg/ml Leupeptin, 10 μg/ml Pepstatin, 10 μg/ml TLCK, and 5 μg/ml TPCK. The crude lysate was clarified and then incubated with anti-*Dd*α-catenin beads, which were prepared by conjugating ammonium sulfate-fractionated antiserum to AminoLink Plus resin (Pierce biotechnology) according to the manufacturer's instructions. Negative control beads were prepared in parallel using the preimmune serum from the same rabbit. The lysate was incubated with anti-*Dd*α-catenin beads for 1 hr at 4°C, washed with lysis buffer, and proteins were eluted in 0.2 M Glycine pH 2.5, 1 mM EDTA.

For mass spectrometry, each sample was loaded in its entirety on a 4%–12% Bis-Tris NuPage gel (Invitrogen) and run until the dye front was 3 cm from the bottom of the wells. The gel was cut into slices corresponding to different molecular weights, and the gel slices were sent to the Harvard Microchemistry and Proteomics Facility (William Lane, director) for in-gel tryptic digestion and LC-MS/MS analysis. Data were returned from the facility as a heat map showing the number of spectral counts detected for each protein in each gel slice. The data were analyzed using custom-written Perl scripts. Proteins identified by only a single unique peptide or by less than three spectral counts were excluded from the analysis, along with obvious contaminants (e.g., keratin) and likely background hits (mitochondrial proteins and other housekeeping enzymes). A partial list of identified proteins is shown in Figure 2B.

Isolation of Triton-Insoluble Cytoskeletons

Cells were developed to culmination, and culminants were dissolved in lysis buffer as described above. The lysates were precleared by centrifuging at 3,000 × g for 10 min. The clarified lysates were then centrifuged at 55,000 rpm for 45 min in a TLA100.1 rotor (Beckman) to pellet Triton-insoluble material. Pellets were resuspended in Laemmli buffer and analyzed by western blotting.

SUPPLEMENTAL INFORMATION

Supplemental Information includes five figures and Supplemental Experimental Procedures and can be found online with this article at http://dx.doi.org/10.1016/j.devcel.2012.06.008.

ACKNOWLEDGMENTS

We thank Jan Faix and Richard Firtel, the Developmental Studies Hybridoma Bank, and the Dictybase Stock Center for reagents; Catherine Carswell-Crumpton for assistance with flow cytometry; William Lane for mass spectrometry; and Bob Goldstein for helpful comments on the manuscript. D.J.D. also wishes to thank Dr. Goldstein for allowing some of the experiments to be completed in his laboratory. This work was supported by an NSF Graduate Research Fellowship (D.J.D.), NIH GM066817 (D.N.R.), NIH GM035527 (W.J.N.) and NIH GM56169 (W.I.W.).

Received: November 10, 2011
Revised: May 1, 2012
Accepted: June 13, 2012
Published online: August 16, 2012

REFERENCES

Adachi, H., Takahashi, Y., Hasebe, T., Shirouzu, M., Yokoyama, S., and Sutoh, K. (1997). Dictyostelium IQGAP-related protein specifically involved in the completion of cytokinesis. J. Cell Biol. *137*, 891–898.

Baker, P.C., and Schroeder, T.E. (1967). Cytoplasmic filaments and morphogenetic movement in the amphibian neural tube. Dev. Biol. *15*, 432–450.

Bhat, P., and Thorn, P. (2009). Myosin 2 maintains an open exocytic fusion pore in secretory epithelial cells. Mol. Biol. Cell *20*, 1795–1803.

Bonner, J.T. (1944). A Descriptive Study of the Development of the Slime Mold Dictyostelium discoideum. Am. J. Bot. *31*, 175–182.

Bonner, J.T., Cihiquoine, A.D., and Kolderie, M.Q. (1955). A histochemical study of differentiation in the cellular slime molds. J. Exp. Zool. *130*, 133–158.

Borghi, N., and Nelson, W.J. (2009). Intercellular adhesion in morphogenesis: molecular and biophysical considerations. Curr. Top. Dev. Biol. *89*, 1–32.

Bryant, D.M., and Mostov, K.E. (2008). From cells to organs: building polarized tissue. Nat. Rev. Mol. Cell Biol. *9*, 887–901.

Coates, J.C., Grimson, M.J., Williams, R.S.B., Bergman, W., Blanton, R.L., and Harwood, A.J. (2002). Loss of the beta-catenin homologue aardvark causes ectopic stalk formation in Dictyostelium. Mech. Dev. *116*, 117–127.

Dawes-Hoang, R.E., Parmar, K.M., Christiansen, A.E., Phelps, C.B., Brand, A.H., and Wieschaus, E.F. (2005). folded gastrulation, cell shape change and the control of myosin localization. Development *132*, 4165–4178.

Dickinson, D.J., Nelson, W.J., and Weis, W.I. (2011). A polarized epithelium organized by beta- and alpha-catenin predates cadherin and metazoan origins. Science *331*, 1336–1339.

Effler, J.C., Kee, Y.-S., Berk, J.M., Tran, M.N., Iglesias, P.A., and Robinson, D.N. (2006). Mitosis-specific mechanosensing and contractile-protein redistribution control cell shape. Curr. Biol. *16*, 1962–1967.

Faix, J., Steinmetz, M., Boves, H., Kammerer, R.A., Lottspeich, F., Mintert, U., Murphy, J., Stock, A., Aebi, U., and Gerisch, G. (1996). Cortexillins, major determinants of cell shape and size, are actin-bundling proteins with a parallel coiled-coil tail. Cell *86*, 631–642.

Faix, J., Clougherty, C., Konzok, A., Mintert, U., Murphy, J., Albrecht, R., Mühlbauer, B., and Kuhlmann, J. (1998). The IQGAP-related protein DGAP1 interacts with Rac and is involved in the modulation of the F-actin cytoskeleton and control of cell motility. J. Cell Sci. *111*, 3059–3071.

Faix, J., Weber, I., Mintert, U., Köhler, J., Lottspeich, F., and Marriott, G. (2001). Recruitment of cortexillin into the cleavage furrow is controlled by Rac1 and IQGAP-related proteins. EMBO J. *20*, 3705–3715.

Fey, P., Kowal, A.S., Gaudet, P., Pilcher, K.E., and Chisholm, R.L. (2007). Protocols for growth and development of Dictyostelium discoideum. Nat. Protoc. *2*, 1307–1316.

Gaudet, P., Pilcher, K.E., Fey, P., and Chisholm, R.L. (2007). Transformation of Dictyostelium discoideum with plasmid DNA. Nat. Protoc. *2*, 1317–1324.

Grimson, M.J., Coates, J.C., Reynolds, J.P., Shipman, M., Blanton, R.L., and Harwood, A.J. (2000). Adherens junctions and beta-catenin-mediated cell signalling in a non-metazoan organism. Nature *408*, 727–731.

Gutzman, J.H., and Sive, H. (2010). Epithelial relaxation mediated by the myosin phosphatase regulator Mypt1 is required for brain ventricle lumen expansion and hindbrain morphogenesis. Development *137*, 795–804.

Kasza, K.E., and Zallen, J.A. (2011). Dynamics and regulation of contractile actin-myosin networks in morphogenesis. Curr. Opin. Cell Biol. *23*, 30–38.

Kee, Y.-S., Ren, Y., Dorfman, D., Iijima, M., Firtel, R., Iglesias, P.A., and Robinson, D.N. (2012). A mechanosensory system governs myosin II accumulation in dividing cells. Mol. Biol. Cell *23*, 1510–1523.

Keller, R. (2002). Shaping the vertebrate body plan by polarized embryonic cell movements. Science *298*, 1950–1954.

Kimberly, E.L., and Hardin, J. (1998). Bottle cells are required for the initiation of primary invagination in the sea urchin embryo. Dev. Biol. *204*, 235–250.

Knecht, D.A., and Loomis, W.F. (1988). Developmental consequences of the lack of myosin heavy chain in Dictyostelium discoideum. Dev. Biol. *128*, 178–184.

Kuroda, S., Fukata, M., Nakagawa, M., Fujii, K., Nakamura, T., Ookubo, T., Izawa, I., Nagase, T., Nomura, N., Tani, H., et al. (1998). Role of IQGAP1, a target of the small GTPases Cdc42 and Rac1, in regulation of E-cadherin-mediated cell-cell adhesion. Science *281*, 832–835.

Lee, J.-Y., and Goldstein, B. (2003). Mechanisms of cell positioning during C. elegans gastrulation. Development *130*, 307–320.

Lee, S., Escalante, R., and Firtel, R.A. (1997). A Ras GAP is essential for cytokinesis and spatial patterning in Dictyostelium. Development *124*, 983–996.

Lee, S., Shen, Z., Robinson, D.N., Briggs, S., and Firtel, R.A. (2010). Involvement of the cytoskeleton in controlling leading-edge function during chemotaxis. Mol. Biol. Cell *21*, 1810–1824.

Li, Z., Kim, S.H., Higgins, J.M., Brenner, M.B., and Sacks, D.B. (1999). IQGAP1 and calmodulin modulate E-cadherin function. J. Biol. Chem. *274*, 37885–37892.

Luo, T., Mohan, K., Srivastava, V., Ren, Y., Iglesias, P.A., and Robinson, D.N. (2012). Understanding the cooperative interaction between myosin II and actin cross-linkers mediated by actin filaments during mechanosensation. Biophys. J. *102*, 238–247.

Martin, A.C., Gelbart, M., Fernandez-Gonzalez, R., Kaschube, M., and Wieschaus, E.F. (2010). Integration of contractile forces during tissue invagination. J. Cell Biol. *188*, 735–749.

Masedunskas, A., Sramkova, M., Parente, L., Sales, K.U., Amornphimoltham, P., Bugge, T.H., and Weigert, R. (2011). Role for the actomyosin complex in regulated exocytosis revealed by intravital microscopy. Proc. Natl. Acad. Sci. USA *108*, 13552–13557.

Meyer, T.N., Schwesinger, C., Bush, K.T., Stuart, R.O., Rose, D.W., Shah, M.M., Vaughn, D.A., Steer, D.L., and Nigam, S.K. (2004). Spatiotemporal regulation of morphogenetic molecules during in vitro branching of the isolated ureteric bud: toward a model of branching through budding in the developing kidney. Dev. Biol. *275*, 44–67.

Nelson, W.J. (2008). Regulation of cell-cell adhesion by the cadherin-catenin complex. Biochem. Soc. Trans. *36*, 149–155.

Newell, P.C., Telser, A., and Sussman, M. (1969). Alternative developmental pathways determined by environmental conditions in the cellular slime mold Dictyostelium discoideum. J. Bacteriol. *100*, 763–768.

Raper, K.B., and Fennell, D.I. (1952). Stalk formation in Dictyostelium. Bull. Torrey Bot. Club *79*, 25–51.

Ren, Y., Effler, J.C., Norstrom, M., Luo, T., Firtel, R.A., Iglesias, P.A., Rock, R.S., and Robinson, D.N. (2009). Mechanosensing through cooperative interactions between myosin II and the actin crosslinker cortexillin I. Curr. Biol. *19*, 1421–1428.

Rot, G., Parikh, A., Curk, T., Kuspa, A., Shaulsky, G., and Zupan, B. (2009). dictyExpress: a Dictyostelium discoideum gene expression database with an explorative data analysis web-based interface. BMC Bioinformatics *10*, 265.

Sawyer, J.M., Harrell, J.R., Shemer, G., Sullivan-Brown, J., Roh-Johnson, M., and Goldstein, B. (2010). Apical constriction: a cell shape change that can drive morphogenesis. Dev. Biol. *341*, 5–19.

Smith, J.L., Silveira, L.A., and Spudich, J.A. (1996). Myosin light chain kinase (MLCK) gene disruption in Dictyostelium: a role for MLCK-A in cytokinesis and evidence for multiple MLCKs. Proc. Natl. Acad. Sci. USA *93*, 12321–12326.

St Johnston, D., and Sanson, B. (2011). Epithelial polarity and morphogenesis. Curr. Opin. Cell Biol. *23*, 540–546.

Surcel, A., Kee, Y.-S., Luo, T., and Robinson, D.N. (2010). Cytokinesis through biochemical-mechanical feedback loops. Semin. Cell Dev. Biol. *21*, 866–873.

Sweeton, D., Parks, S., Costa, M., and Wieschaus, E. (1991). Gastrulation in Drosophila: the formation of the ventral furrow and posterior midgut invaginations. Development *112*, 775–789.

Weber, I., Gerisch, G., Heizer, C., Murphy, J., Badelt, K., Stock, A., Schwartz, J.M., and Faix, J. (1999). Cytokinesis mediated through the recruitment of cortexillins into the cleavage furrow. EMBO J. *18*, 586–594.

Weijer, C.J. (2004). Dictyostelium morphogenesis. Curr. Opin. Genet. Dev. *14*, 392–398.

Yamashiro, S., Abe, H., and Mabuchi, I. (2007). IQGAP2 is required for the cadherin-mediated cell-to-cell adhesion in Xenopus laevis embryos. Dev. Biol. *308*, 485–493.

Developmental Cell, Volume *23*

Supplemental Information

α-Catenin and IQGAP Regulate Myosin Localization to Control Epithelial Tube Morphogenesis in *Dictyostelium*

Daniel J. Dickinson, Douglas N. Robinson, W. James Nelson, and William I. Weis

Inventory of Supplemental Information

Supplemental information includes supplemental experimental procedures and five supplemental figures.

Supplemental Experimental Procedures include detailed descriptions of strains, plasmids, antibodies, cell culture and transformation and quantitative image analysis methods that are summarized in the main text.

The five Supplemental Figures are related to main Figures 1, 2, 3, 4 and 6, as follows:

- Figure S1, related to Figure 1: Myosin and GFP-myosin expression levels in cell lines used in this study
- Figure S2, related to Figure 2: Illustration of our procedure for quantifying GFP-myosin distribution
- Figure S3, related to Figure 3: Domain structures of IQGAPs and cortexillins
- Figure S4, related to Figure 4: Range of phenotypes observed in *ctxA*- culminants
- Figure S5, related to Figure 6: Myosin is excluded from the cortex in severe α-catenin knockdowns

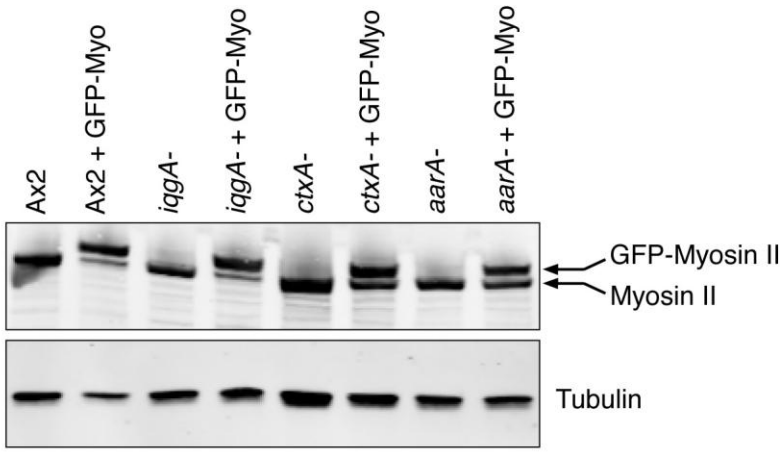

Figure S1, related to Figure 1: Myosin and GFP-myosin expression levels in cell lines used in this study

Lysates of the indicated cells were separated on SDS-PAGE gels and analyzed by western blotting with anti-myosin (top) or anti-α-tubulin (bottom) antibodies.

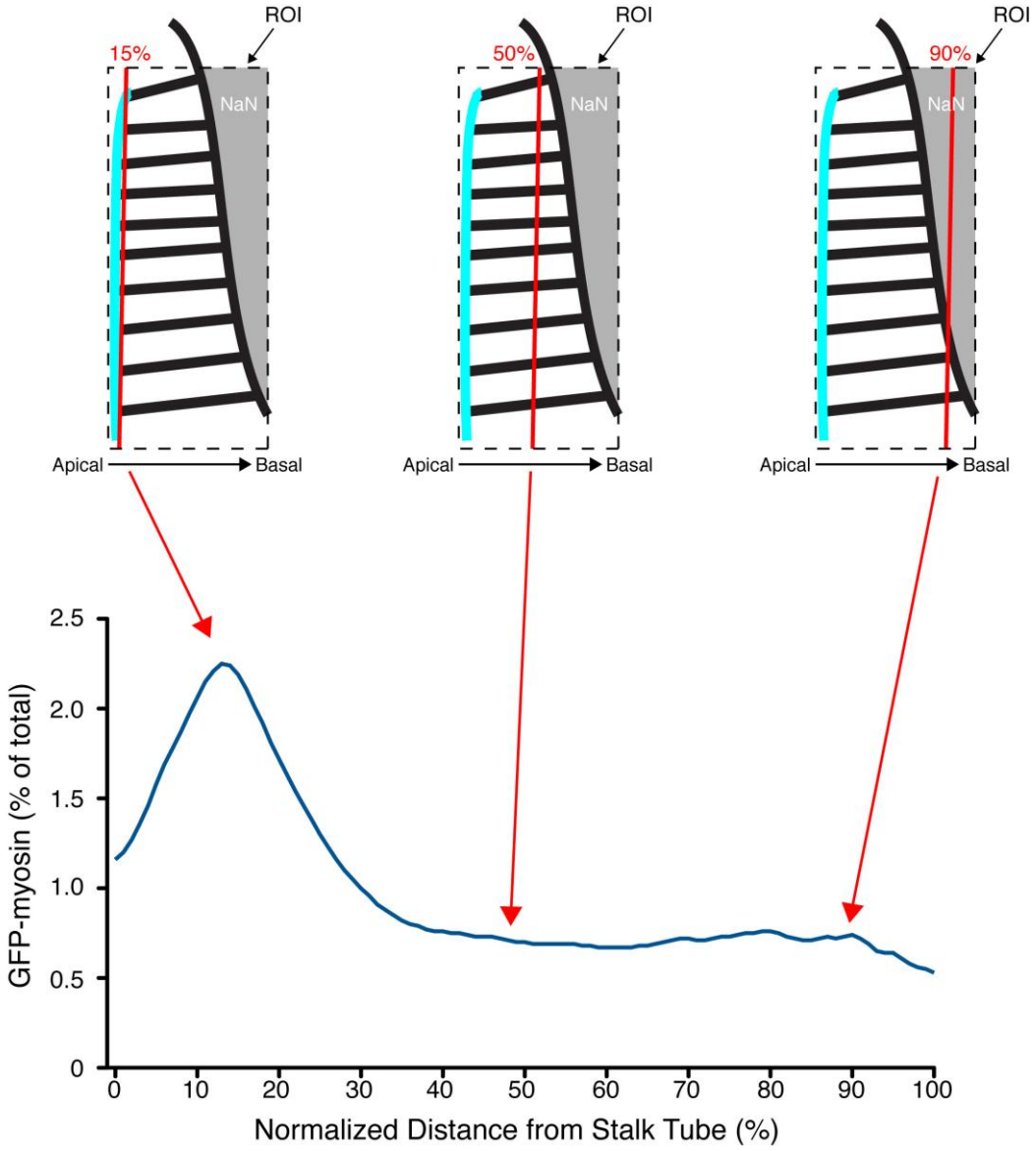

Figure S2, related to Figure 2: Illustration of our procedure for quantifying GFP-myosin distribution

A region of interest comprising the tip epithelium was selected (dashed rectangle). A 1 pixel wide line parallel to the stalk tube (red line) was scanned across this ROI, and average GFP-myosin intensity along the line at each point was measured. Regions outside the tip (gray) were selected using a low pixel intensity threshold, set to NaN, and ignored by the algorithm. The resulting intensity profile is equivalent to taking line scans at each point perpendicular to the stalk tube, and averaging the results.

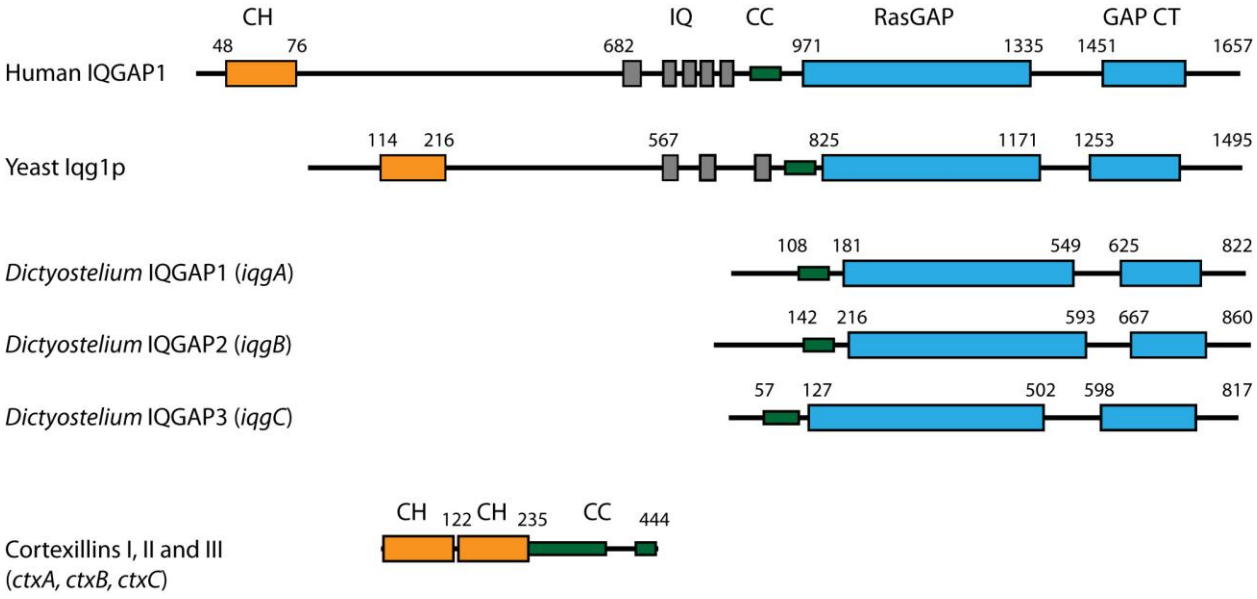

Figure S3, related to Figure 3: Domain structures of IQGAPs and cortexillins

Stick diagrams show the domains present in each protein. Numbers indicate amino acid residues. Abbreviations: CH, calponin homology (an actin-binding domain); IQ, IQ motif; CC, coiled-coil motif; RasGAP, RasGAP-like domain (note that IQGAPs do not have GTPase-activating activity (Faix et al., 1998)); GAP CT, RasGAP C-terminal domain.

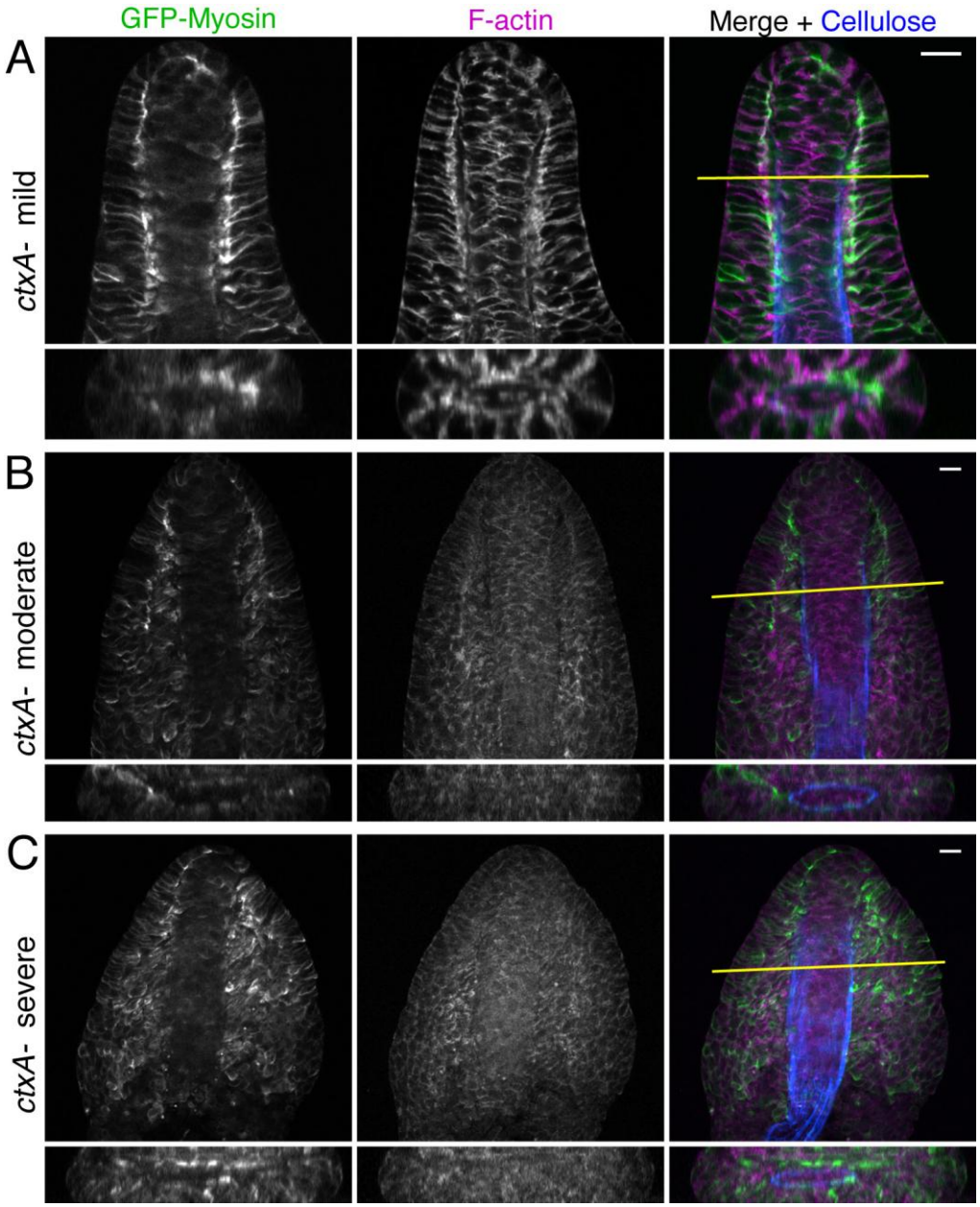

Figure S4, related to Figure 4: Range of phenotypes observed in *ctxA*- culminants

Confocal sections of the tips of three different *ctxA*- culminants expressing GFP-myosin and stained for F-actin and cellulose, illustrating the range of phenotypes observed in this strain. Lower panels show cross sections at the planes indicated by the yellow lines. Images in panel (B) are representative of the majority of cases and are the same as those shown in figure 4B. Scale bars represent 10 μm.

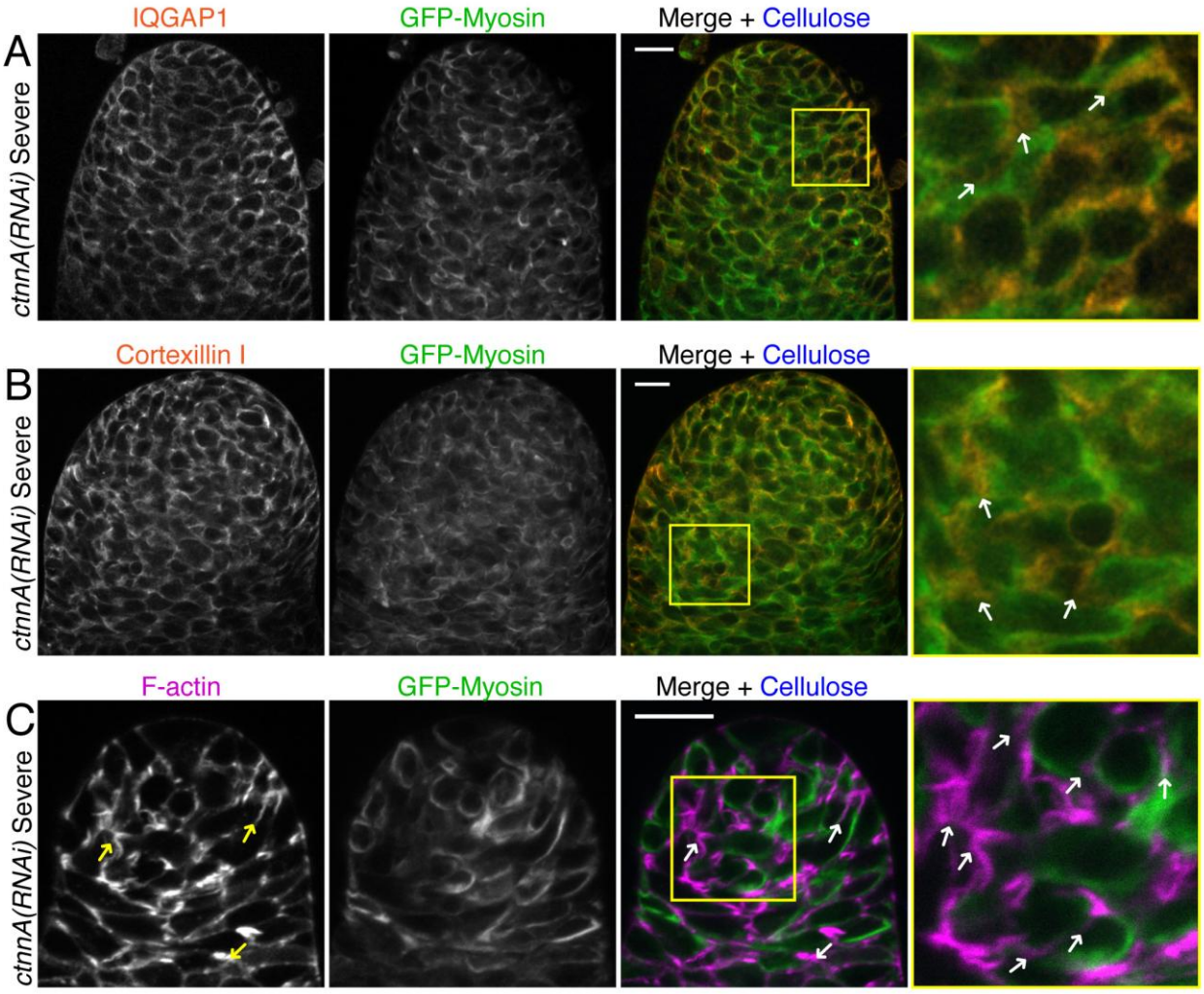

Figure S5, related to Figure 6: Myosin is excluded from the cortex in severe α-catenin knockdowns

(A-C) Confocal sections of the tips of *ctnnA(RNAi)* culminants showing the severe phenotype, stained as indicated. The far right panels show enlargements of the boxed regions. Arrows indicate cortical regions that are devoid of GFP-myosin.

Scale bars represent 10 μm.

Supplemental Experimental Procedures

Strains, plasmids and antibodies

Dictyostelium discoideum strain Ax2 was used as wild-type. *aarA*- (Grimson et al., 2000), *mlkA*- (Smith et al., 1996) and *ctxA*- cells (Faix et al., 1996) were obtained from the Dictybase stock center; *iqgA*- cells (Lee et al., 1997) were a gift from Richard A. Firtel (University of California, San Diego, CA). All cell lines were maintained as spore stocks and were passaged for no more than 3 weeks in axenic culture before use in experiments.

GFP-myosin was expressed using a previously described pDRH vector (Effler et al., 2006). GFP-myosin expressing cells were FACS sorted to obtain homogenous and consistent expression levels. mRFP-dcsA was expressed under the control of its own promoter as previously described (Dickinson et al., 2011). α-Catenin was depleted by expressing a long double-stranded RNA under the control of a doxycycline-inducible promoter, as previously described (Dickinson et al., 2011).

The following antibodies were used in this study: anti-α-catenin antiserum has been described previously (Dickinson et al., 2011); mAb 216-394-1 recognizing IQGAP1 and mAb 241-36-2 recognizing cortexillin I in immunofluorescence experiments were gifts from Jan Faix (Hannover Medical School, Hannover, Germany); mAb 232-238-10 recognizing cortexillin II, mAb 12G10 recognizing α-tubulin, mAb 241-438-1 recognizing cortexillin I in western blots and mAb 21-55-4 recognizing myosin heavy chain were from the Developmental Studies Hybridoma Bank; anti-actin for western blotting was from Sigma.

Cell culture and transformation

Dictyostelium discoideum cells were grown in HL5 medium (7 g/L Proteose Peptone #2 (BD Biosciences), 7 g/L Proteose Peptone #3 (BD Biosciences), 7 g/L yeast extract, 13.5 g/L glucose, 1.5 g/L KH_2PO_4, 0.5 g/L Na_2HPO_4, pH 6.5) supplemented with penicillin, streptomycin and kanamycin to prevent bacterial growth. Cells were passaged at least every third day and were maintained in axenic culture for no more than 3 weeks before fresh cells were started from spore stocks.

For transformation, cells were washed three times with ice-cold electroporation buffer H-50 (20 mM HEPES, 50 mM KCl, 10 mM NaCl, 1 mM $MgSO_4$, 5 mM $NaHCO_3$, 10 mM

Na_2HPO_4, pH 7.0), counted, and resuspended in H-50 at a density of 10^7 cells per 300 μL. 300 μL cells were mixed with 10 μg plasmid DNA in a 0.4 cm electroporation cuvette and treated with two 1 ms square wave pulses at 1000 V, with 5 seconds between pulses, in a Bio-Rad Gene Pulser XCell electroporation system. 800 μL chilled HL5 medium was immediately added and the cells were allowed to recover on ice for several minutes before transferring to culture dishes containing selection-free medium. Selection drugs were added the next day, and the medium was then changed every other day until colonies appeared (routinely 4-7 days). For selection, we used 60 μg/mL hygromycin, 10 μg/mL G418, or a combination of 60 μg/mL hygromycin and 20 μg/mL G418.

Measurement of stalk tube width

We chose to report cross-sectional area of the stalk tube (rather than diameter or radius) because stalk tubes did not always remain cylindrical through the fixation and mounting process, especially in some of the mutant strains. To measure stalk tube cross-sectional area, a confocal series was obtained through an entire tip. The 3D image was analyzed in ImageJ as follows: 1) An XZ image was created from the confocal stack at a plane perpendicular to the long axis of the stalk and at the center (in the vertical direction) of the tip epithelium; 2) The cellulose channel was thresholded and skeletonized (or traced manually where necessary) to obtain an outline of the stalk tube cross-section; 3) The area of this shape was measured using the "fill holes" command followed by measurement of integrated density (which gives the total positive area for a binary image). Values in the text are reported as mean area ± SEM.

Quantification of protein localization

Our procedure for quantifying GFP-myosin distribution (Figures 2C and 4C) is illustrated in Supplemental Figure S2. We first defined a region of interest comprising the entire tip epithelium in a single confocal image. The average GFP pixel intensity was then measured along 1 pixel wide lines parallel to the stalk tube, using a custom-written script in ImageJ. The resulting intensity profile is analogous to a line scan along a line perpendicular to the stalk tube, except that each point corresponds the average pixel intensity at all points located a given distance from the stalk tube, rather than to a single intensity value. To enable averaging and comparison across multiple images, the distance from the stalk tube (x-axis) was normalized to

the total height of each tip epithelium, and the myosin intensity (y-axis) was expressed as a percentage of the total intensity in the entire tip epithelium.

To measure IQGAP1 and cortexillin I localization, average pixel intensities were measured along 5 pixel wide lines encompassing the apical (adjacent to the stalk tube) and basal (exterior of the culminant) plasma membranes. To avoid bias, these lines were drawn while viewing in the F-actin channel. IQGAP1 and cortexillin I distributions were expressed as an apical:basal intensity ratio to control for variable staining. To avoid artifacts, images in which antibody staining appeared incomplete (as judged by the absence of a signal in the stalk cells) were excluded from the analysis.

To quantify the anti-correlated localizations of IQGAP1 and GFP-myosin, we defined a region of interest comprising the entire tip epithelium in a single confocal image. The images were thresholded to remove off-culminant and cytoplasmic background; the exact choice of the threshold value did not qualitatively affect the results. GFP and IQGAP1 signal intensities were then measured for each above-threshold pixel, and Spearmann's rank correlation coefficient was calculated. The mean, 95% confidence intervals and p-values reported in Figures 5E and 6G were calculated using the Fisher r-to-z transformation.

To measure lateral cortical localization of α-catenin at lateral cell-cell contacts, we defined a linear region of interest parallel to the basal membrane and passing approximately through the center of the lateral membranes of the tip epithelial cells. The exact choice of the region of interest did not qualitatively affect the results. Signal intensities of α-catenin and F-actin (a marker for the cortex) were measured at each pixel along this line, and Spearmann's rank correlation coefficient was calculated. The mean, 95% confidence intervals and p-values reported in Figure 7B were calculated using the Fisher r-to-z transformation. Because our region of interest included both cortex and cytosol, higher values of the correlation coefficient indicate enrichment of α-catenin the lateral membrane relative to the cytosol. This cross-correlation method was used (as opposed to directly measuring pixel intensity) because 1) it does not depend on absolute signal levels and thus enabled comparison of samples across multiple experiments, and 2) it allowed us to measure all of the cell-cell contacts along the linear region of interest and avoided the bias that would have been introduced by selecting individual cell-cell contacts for measurement.